The impact of Galactic DM on annihilation signals from Sagittarius (and other dwarfs)

Evan Vienneau

Department of Physics

University of Alberta

Based on **arXiv:2403.15544** and **arXiv:2509.05519**

In Collaboration with N. Bozorgnia (supervisor), L. Strigari, O. Hartl, E. Batteas and A. Evans

Sagittarius Dwarf Spheroidal

- The Sagittarius (Sgr) dwarf spheroidal is a nearby DM dominated galaxy
- Significant tidal disruption
- Hosts a population of globular clusters

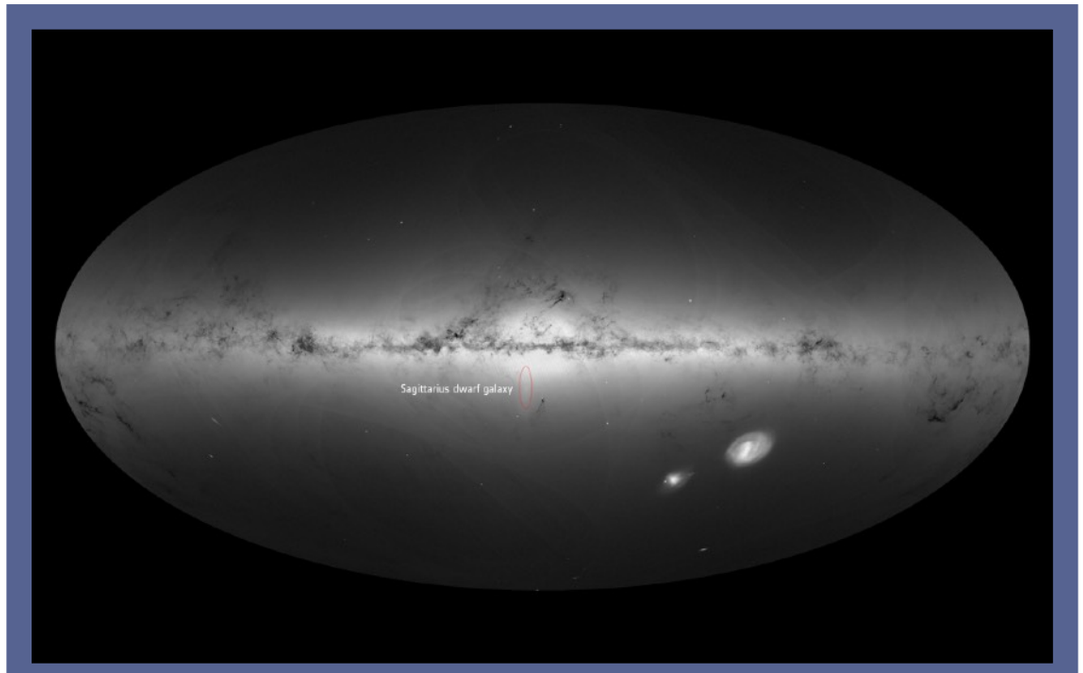

Sagittarius Dwarf Spheroidal

- The Sagittarius (Sgr) dwarf spheroidal is a nearby DM dominated galaxy
- Significant tidal disruption
- Hosts a population of globular clusters

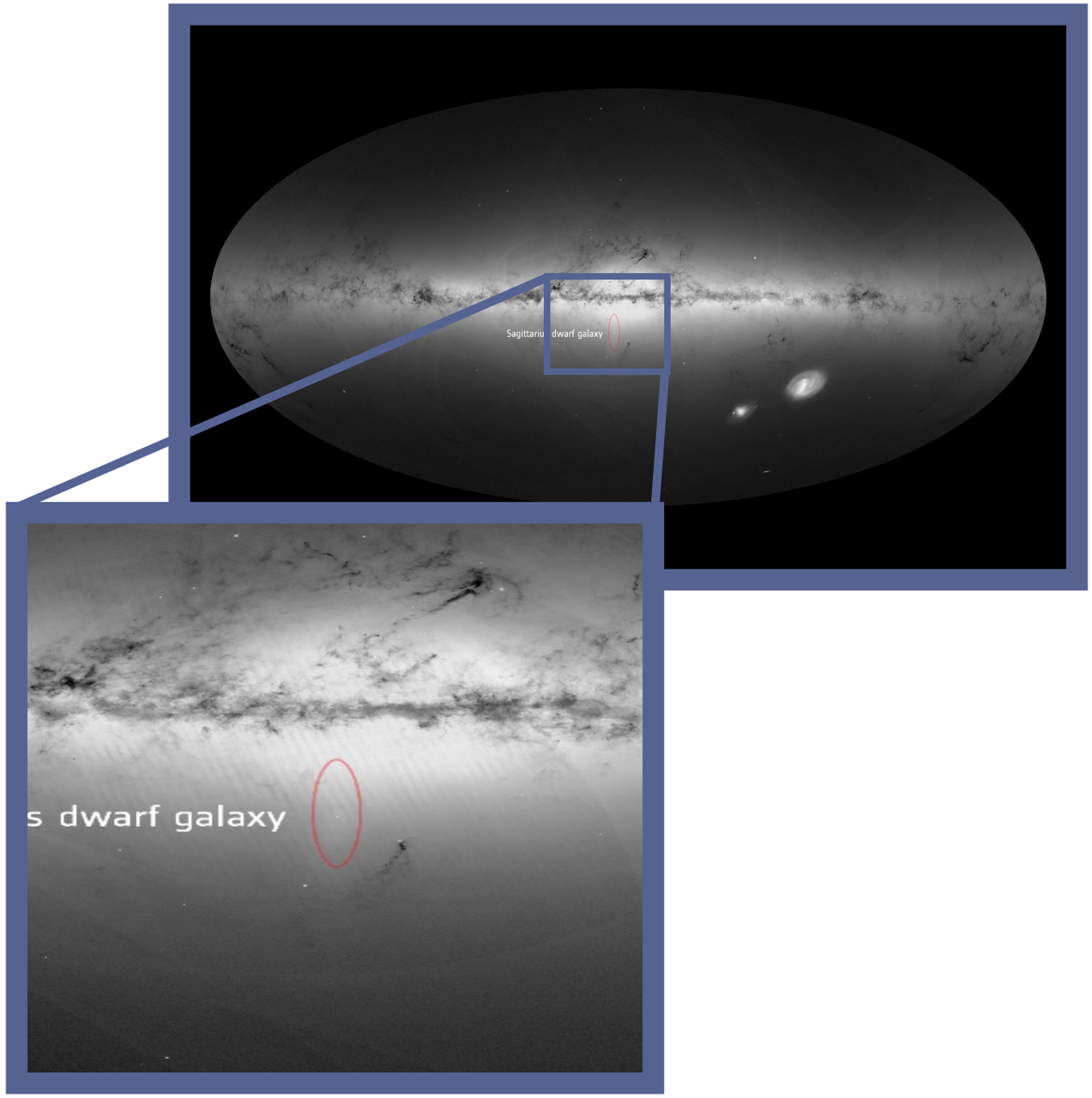

Sagittarius Dwarf Spheroidal

- The Sagittarius (Sgr) dwarf spheroidal is a nearby DM dominated galaxy
- Significant tidal disruption
- Hosts a population of globular clusters
- A gamma-ray source has been identified in the core, is it DM or MSPs?
- Simulations are necessary to extract DM distribution

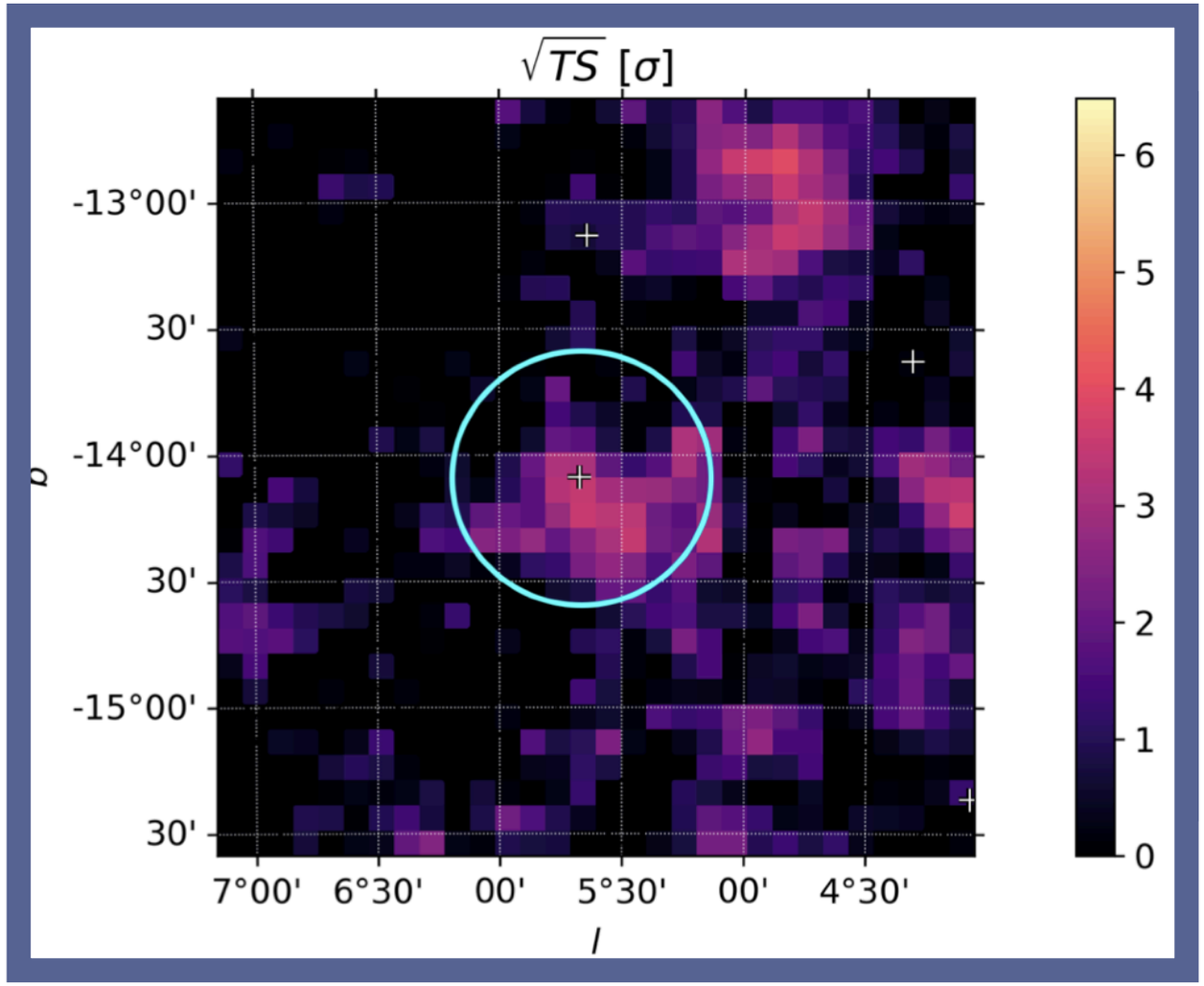

[Evans et al. 22']

Simulated Sgr Analogues

- Auriga is a suite of magneto-hydrodynamical zoom-in simulations of MW analogues

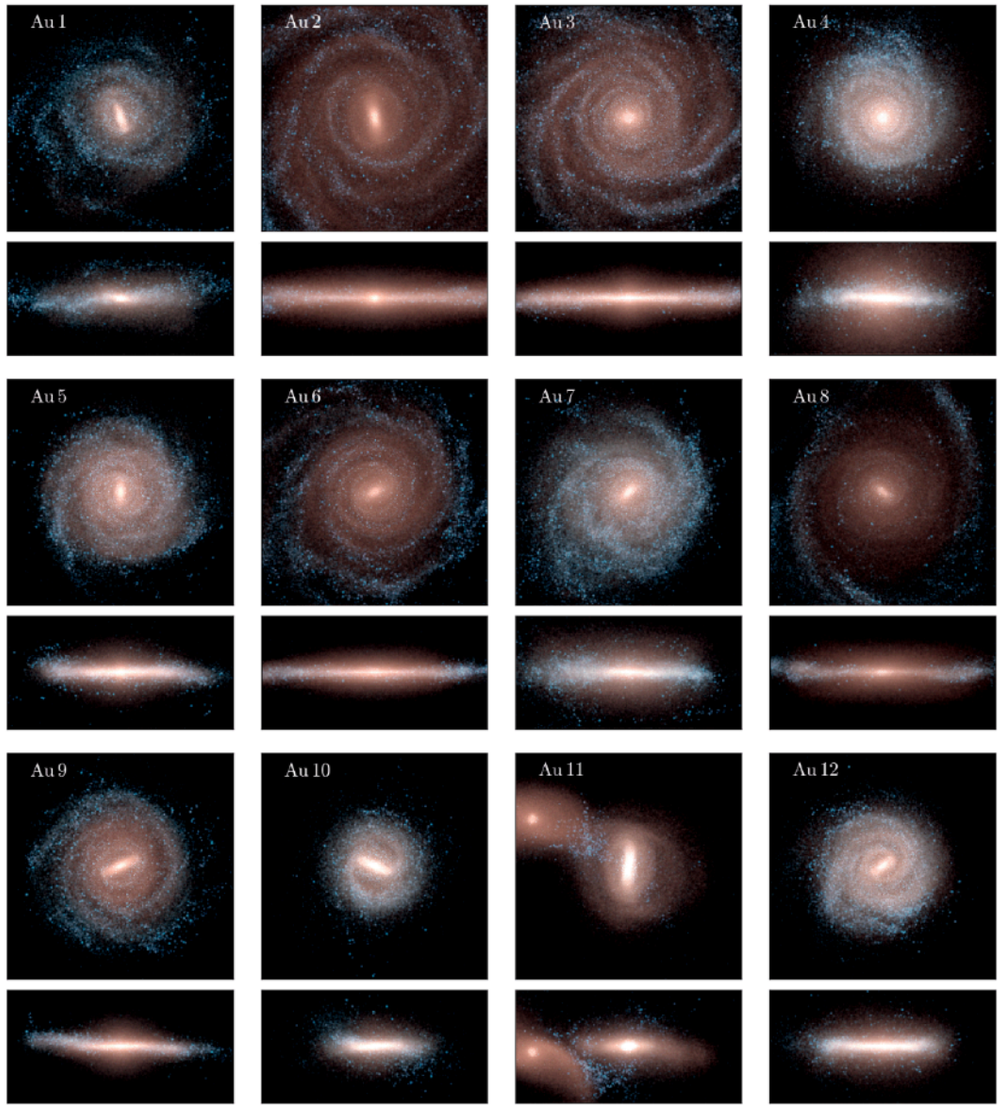

[Grand et al. 16']

Simulated Sgr Analogues

- Auriga is a suite of magneto-hydrodynamical zoom-in simulations of MW analogues
- Six Sgr analogues are identified by matching bound stellar mass and galactocentric distance to observations

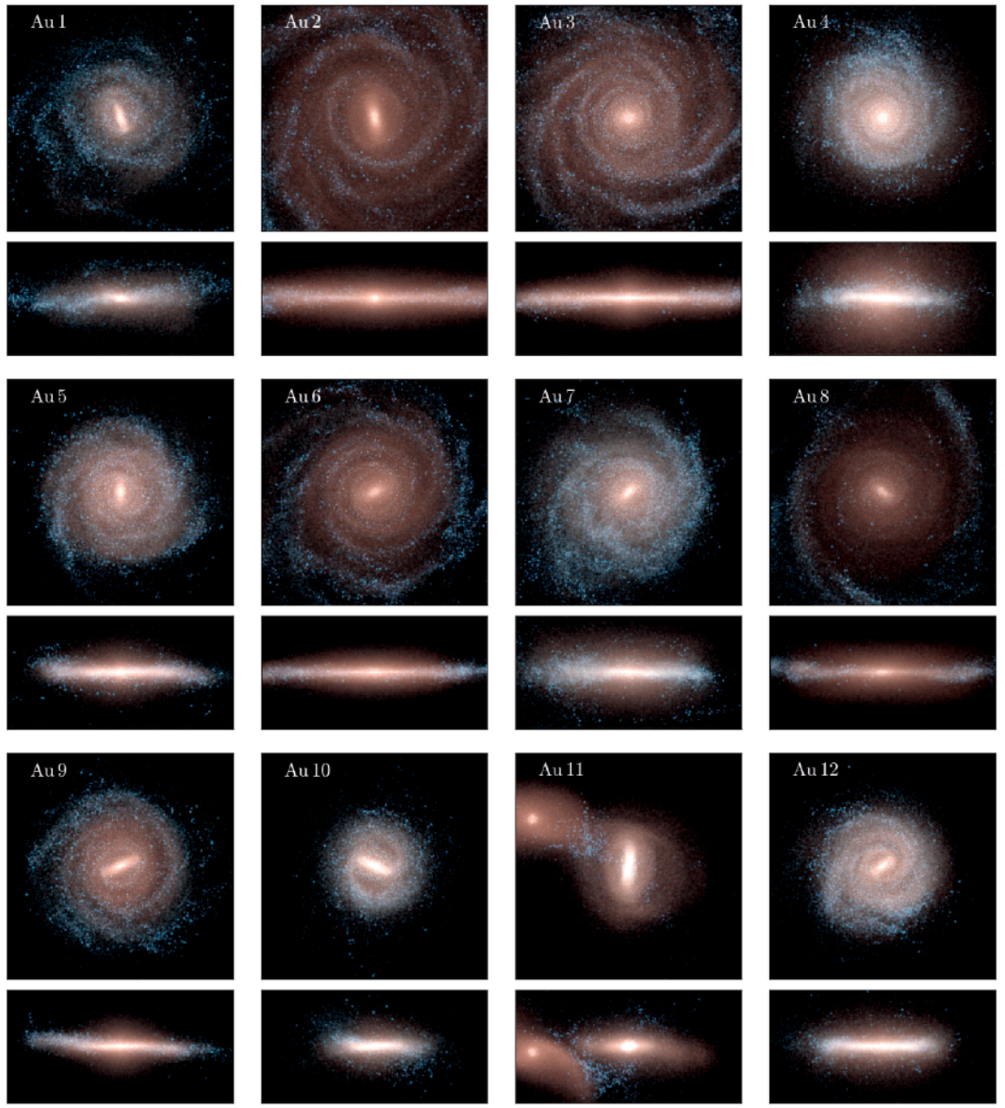

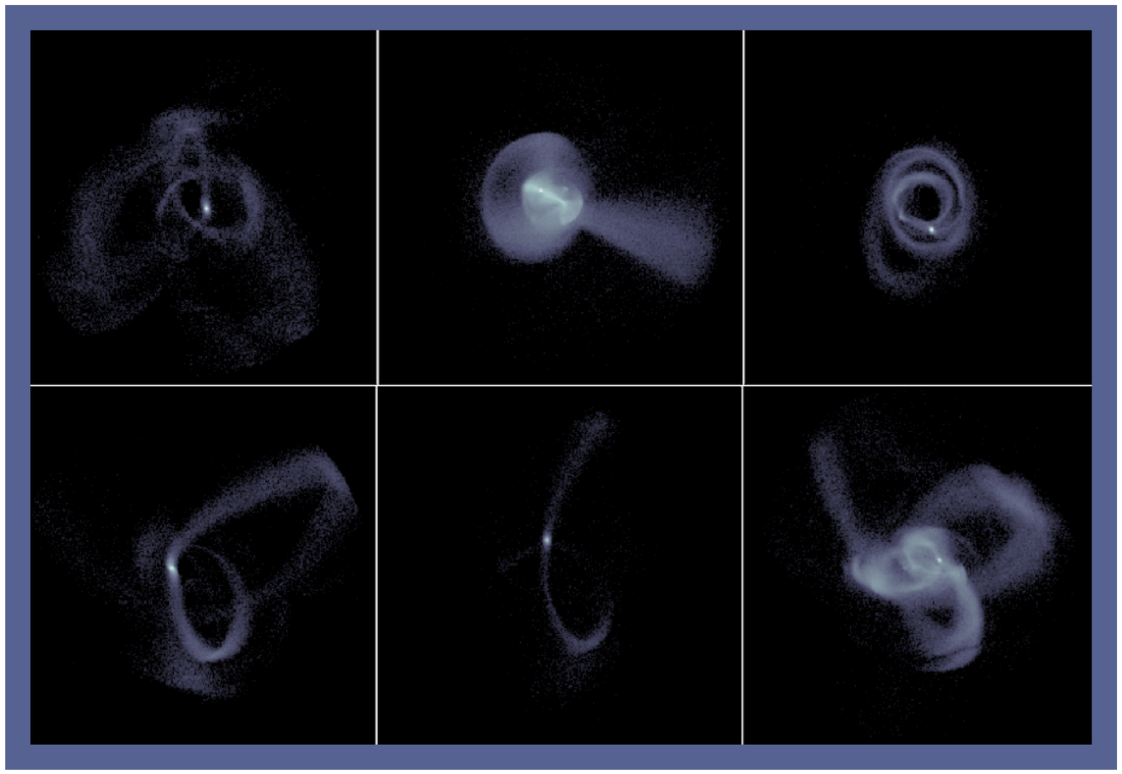

[Grand et al. 16']

Indirect Detection J-Factor

$$\frac{d\Phi_\gamma}{dE} = \frac{(\sigma_A v_{\rm rel})_0}{8\pi m_\chi^2} \frac{dN_\gamma}{dE} \int d\ell \int d^3\mathbf{v}_{\rm rel} P_{\mathbf{x}}(\mathbf{v}_{\rm rel}) \left(\frac{v_{\rm rel}}{c}\right)^n [\rho(r(\ell,\theta))]^2$$

Indirect Detection J-Factor

$$\frac{d\Phi_\gamma}{dE} = \frac{(\sigma_A v_{\rm rel})_0}{8\pi m_\chi^2} \frac{dN_\gamma}{dE} \boxed{\int d\ell \int d^3\mathbf{v}_{\rm rel} P_{\mathbf{x}}(\mathbf{v}_{\rm rel}) \left(\frac{v_{\rm rel}}{c}\right)^n [\rho(r(\ell,\theta))]^2}$$

J-Factor

Indirect Detection J-Factor

$$\frac{d\Phi_\gamma}{dE} = \frac{(\sigma_A v_{\rm rel})_0}{8\pi m_\chi^2} \frac{dN_\gamma}{dE} \boxed{\int d\ell \int d^3\mathbf{v}_{\rm rel} P_{\mathbf{x}}(\mathbf{v}_{\rm rel}) \left(\frac{v_{\rm rel}}{c}\right)^n [\rho(r(\ell,\theta))]^2}$$

J-Factor

- DM density

$$[\rho(\mathbf{x})]^2$$

- n-th moment of relative velocity distribution

$$\mu_n(\mathbf{x}) = \int d^3\mathbf{v}_{\rm rel} P_{\mathbf{X}}(\mathbf{v}_{\rm rel}) \left(\frac{v_{\rm rel}}{c}\right)^n$$

Indirect Detection J-Factor

$$\frac{d\Phi_\gamma}{dE} = \frac{(\sigma_A v_{\rm rel})_0}{8\pi m_\chi^2} \frac{dN_\gamma}{dE} \boxed{\int d\ell \int d^3\mathbf{v}_{\rm rel} P_{\mathbf{x}}(\mathbf{v}_{\rm rel}) \left(\frac{v_{\rm rel}}{c}\right)^n [\rho(r(\ell,\theta))]^2}$$

J-Factor

- DM density

$$[\rho(\mathbf{x})]^2$$

- n-th moment of relative velocity distribution

$$\mu_n(\mathbf{x}) = \int d^3\mathbf{v}_{\rm rel} P_{\mathbf{x}}(\mathbf{v}_{\rm rel}) \left(\frac{v_{\rm rel}}{c}\right)^n$$

S-wave (ℓ = 0, n = 0)

Indirect Detection J-Factor

$$\frac{d\Phi_\gamma}{dE} = \frac{(\sigma_A v_{\rm rel})_0}{8\pi m_\chi^2} \frac{dN_\gamma}{dE} \boxed{\int d\ell \int d^3\mathbf{v}_{\rm rel} P_{\mathbf{x}}(\mathbf{v}_{\rm rel}) \left(\frac{v_{\rm rel}}{c}\right)^n [\rho(r(\ell,\theta))]^2}$$

J-Factor

- DM density

$$[\rho(\mathbf{x})]^2$$

- n-th moment of relative velocity distribution

$$\mu_n(\mathbf{x}) = \int d^3\mathbf{v}_{\rm rel} P_{\mathbf{x}}(\mathbf{v}_{\rm rel}) \left(\frac{v_{\rm rel}}{c}\right)^n$$

S-wave (ℓ = 0, n = 0)

P-wave (ℓ = 1, n = 2) , e.g. Majorana spin 1/2

[Kumar & Marfatia 13']

Indirect Detection J-Factor

$$\frac{d\Phi_\gamma}{dE} = \frac{(\sigma_A v_{\rm rel})_0}{8\pi m_\chi^2} \frac{dN_\gamma}{dE} \boxed{\int d\ell \int d^3\mathbf{v}_{\rm rel} P_{\mathbf{x}}(\mathbf{v}_{\rm rel}) \left(\frac{v_{\rm rel}}{c}\right)^n [\rho(r(\ell,\theta))]^2}$$

J-Factor

- DM density

$$[\rho(\mathbf{x})]^2$$

- n-th moment of relative velocity distribution

$$\mu_n(\mathbf{x}) = \int d^3\mathbf{v}_{\rm rel} P_{\mathbf{x}}(\mathbf{v}_{\rm rel}) \left(\frac{v_{\rm rel}}{c}\right)^n$$

S-wave (ℓ = 0, n = 0)

P-wave (ℓ = 1, n = 2) , e.g. Majorana spin 1/2

[Kumar & Marfatia 13']

D-wave (ℓ = 2, n = 4) , e.g. real scalar

[Giacchino 13']

Indirect Detection J-Factor

$$\frac{d\Phi_\gamma}{dE} = \frac{(\sigma_A v_{\rm rel})_0}{8\pi m_\chi^2} \frac{dN_\gamma}{dE} \boxed{\int d\ell \int d^3\mathbf{v}_{\rm rel} P_{\mathbf{x}}(\mathbf{v}_{\rm rel}) \left(\frac{v_{\rm rel}}{c}\right)^n [\rho(r(\ell,\theta))]^2}$$

J-Factor

- DM density

$$[\rho(\mathbf{x})]^2$$

- n-th moment of relative velocity distribution

$$\mu_n(\mathbf{x}) = \int d^3\mathbf{v}_{\rm rel} P_{\mathbf{x}}(\mathbf{v}_{\rm rel}) \left(\frac{v_{\rm rel}}{c}\right)^n$$

S-wave (ℓ = 0, n = 0)

P-wave (ℓ = 1, n = 2) , e.g. Majorana spin 1/2

[Kumar & Marfatia 13']

D-wave (ℓ = 2, n = 4) , e.g. real scalar

[Giacchino 13']

Sommerfeld (n = -1) , long range interaction

[Feng 10']

Sgr J-Factors

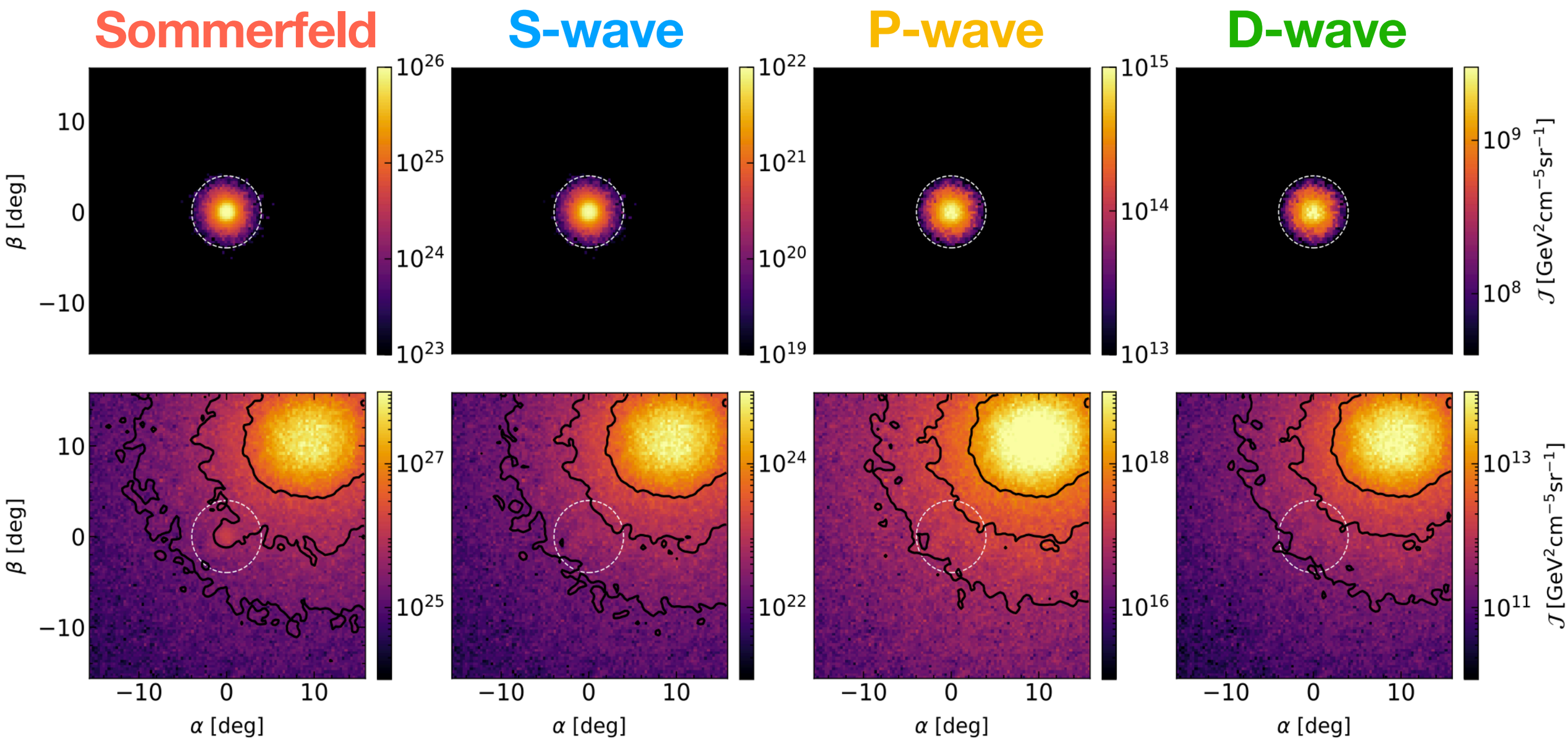

Sgr J-Factors

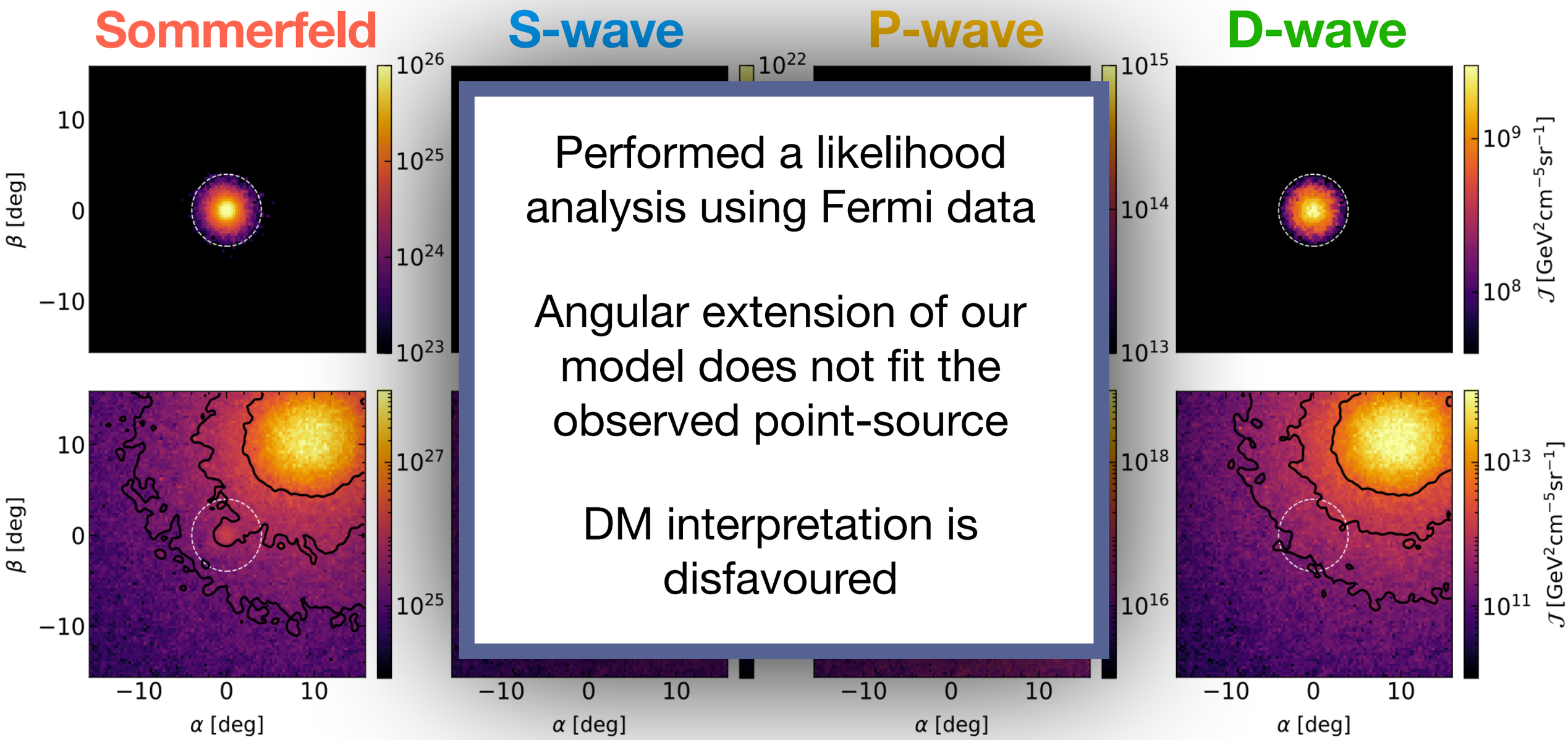

Performed a likelihood analysis using Fermi data

Angular extension of our model does not fit the observed point-source

DM interpretation is disfavoured

Impact of unbound MW DM

- There are two populations of DM within a subhalo:
  - **DM that is bound to the subhalo**

Density Profiles

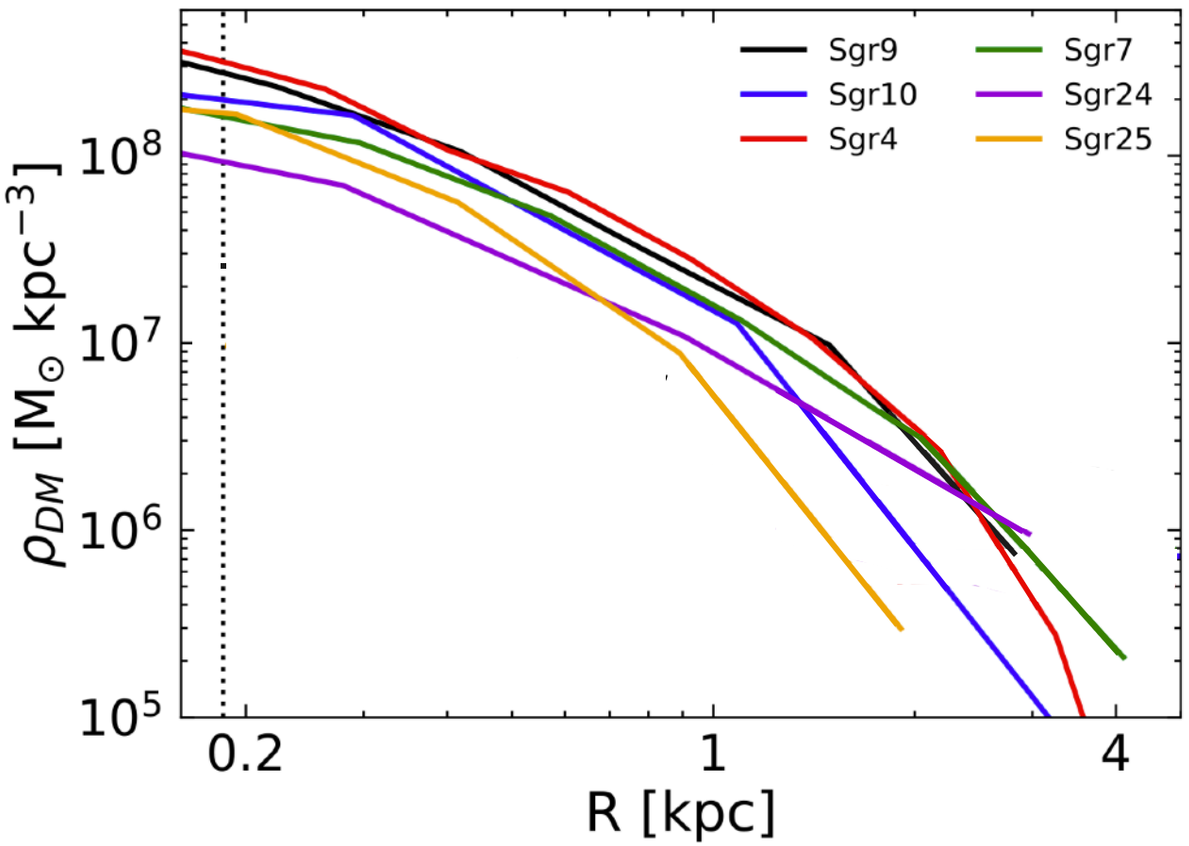

Relative Velocity Distribution

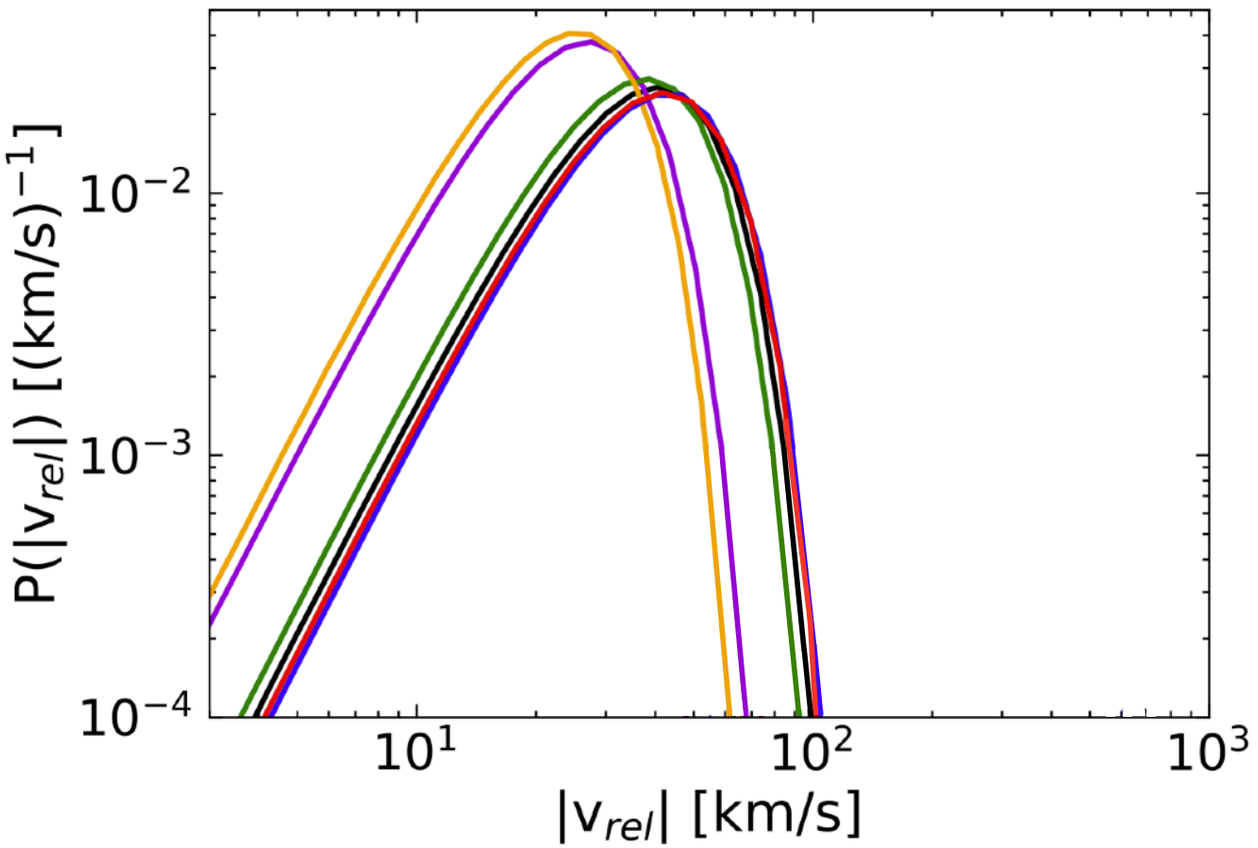

Impact of unbound MW DM

- There are two populations of DM within a subhalo:
  - DM that is bound to the subhalo
  - **DM that is bound to the MW (not bound to subhalo)**

Density Profiles

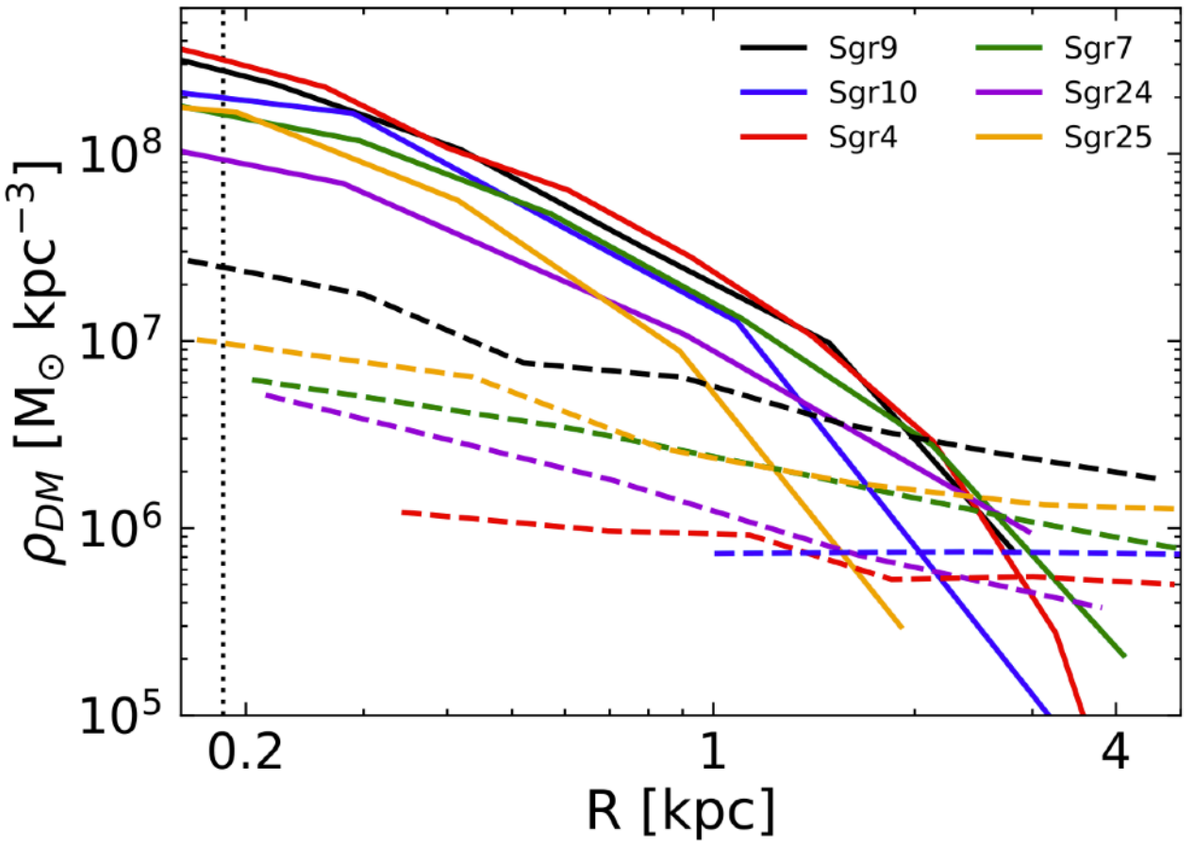

Relative Velocity Distribution

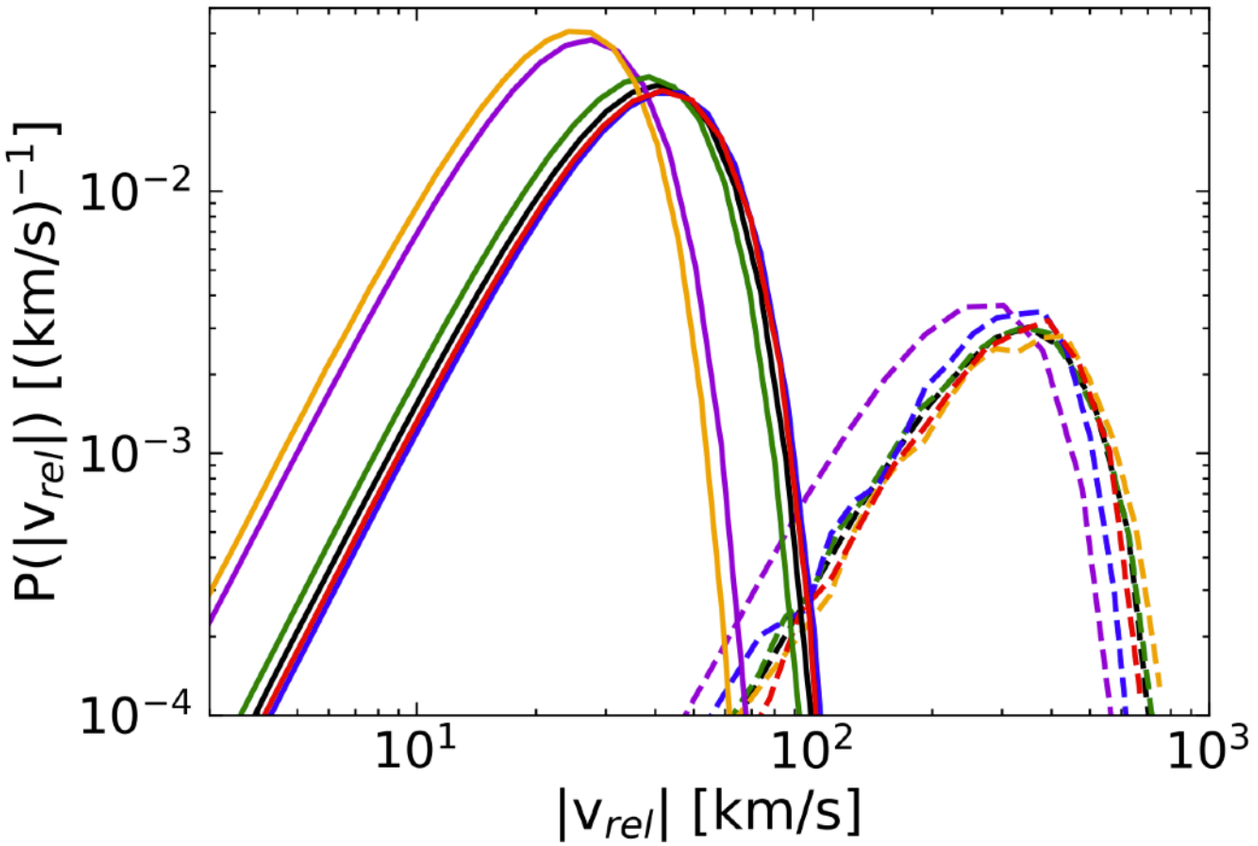

Impact of unbound MW DM

- There are two populations of DM within a subhalo:
  - DM that is bound to the subhalo
  - **DM that is bound to the MW (not bound to subhalo)**

Density Profiles

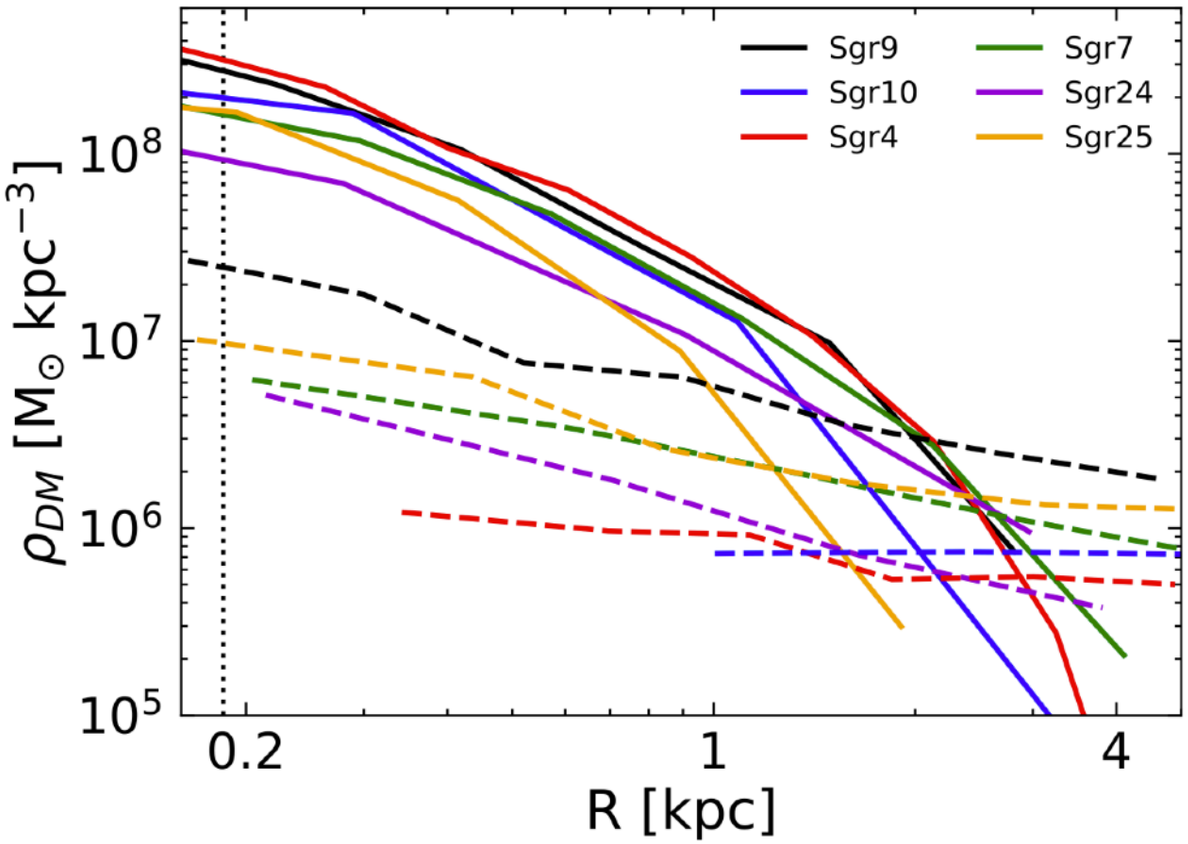

Relative Velocity Distribution

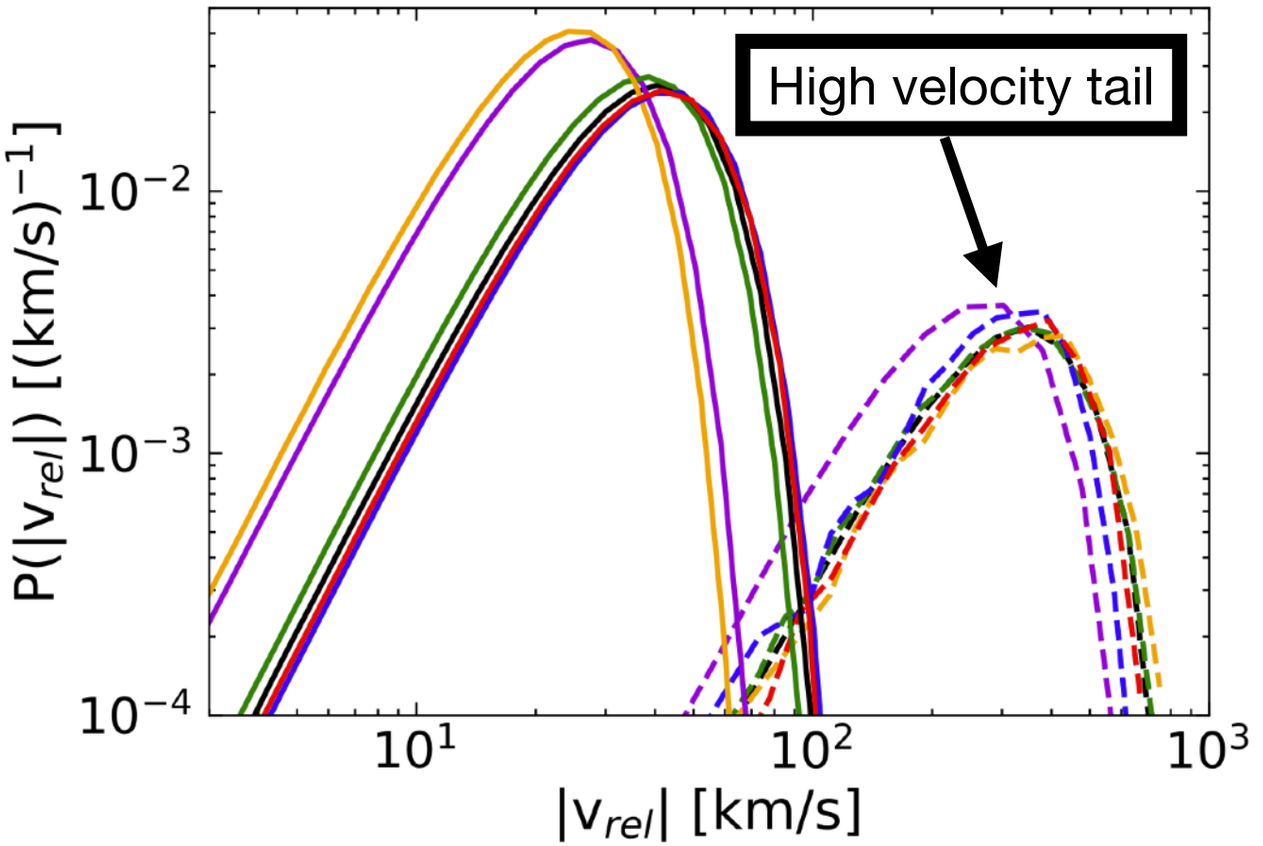

Impact of unbound MW DM

- There are two populations of DM within a subhalo:
  - DM that is bound to the subhalo
  - **DM that is bound to the MW (not bound to subhalo)**

Density Profiles

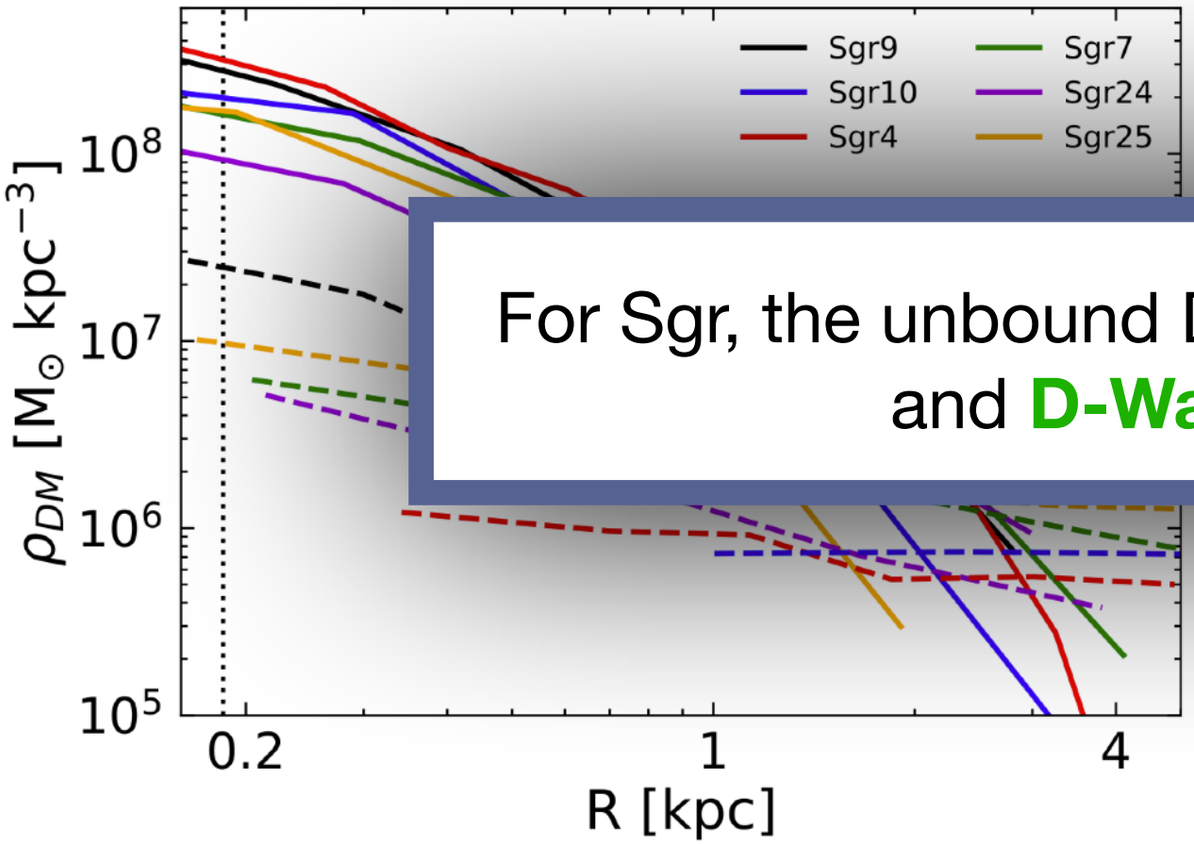

Relative Velocity Distribution

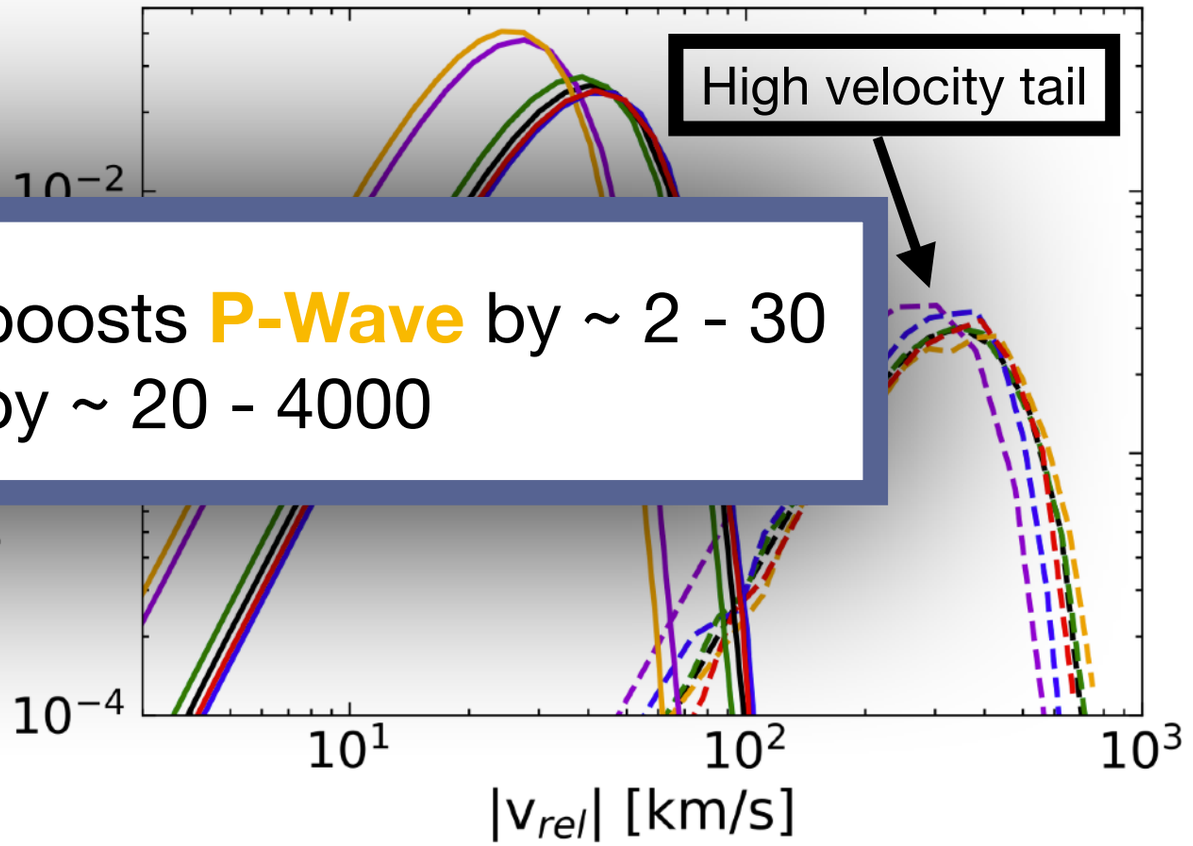

For Sgr, the unbound DM boosts **P-Wave** by ~ 2 - 30 and **D-Wave** by ~ 20 - 4000

Further Quantifying the Boost

- In a follow up study, we investigated this boost for ~ 900 resolved subhalos from the Auriga simulations

Further Quantifying the Boost

- In a follow up study, we investigated this boost for ~ 900 resolved subhalos from the Auriga simulations
- Identified the correlation with galactocentric distance

P-wave

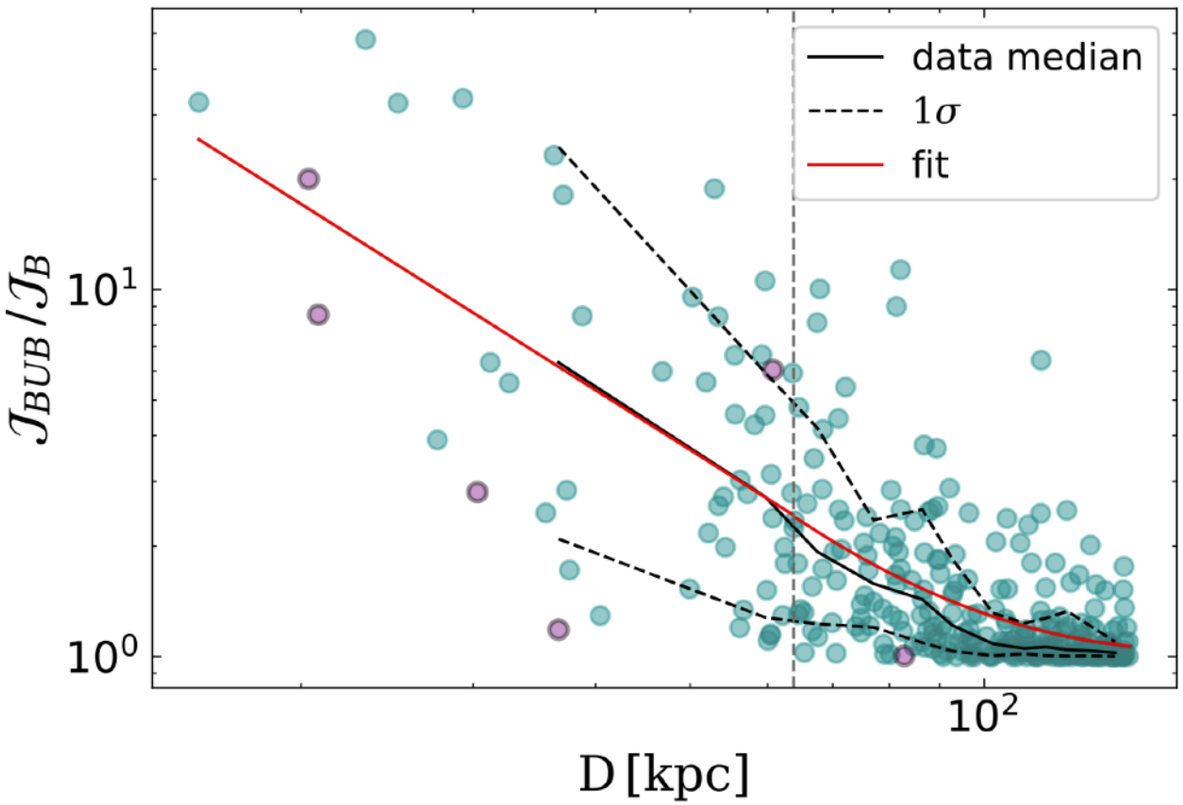

D-wave

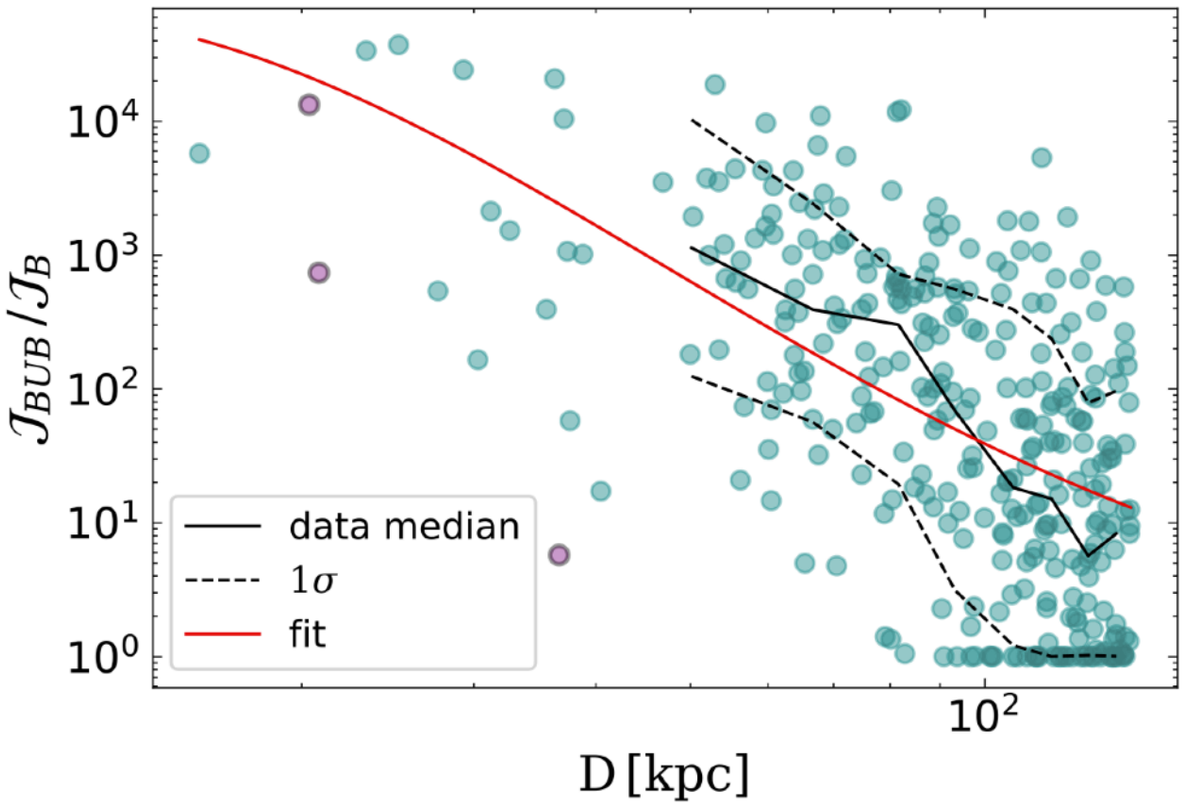

Impact on Exclusion Limits

- Determined the predicted boost for **Ursa Major II** and **Segue I**
- Recomputed **P-Wave** and **D-Wave** exclusion limits, taking into account unbound MW DM particles

P-wave

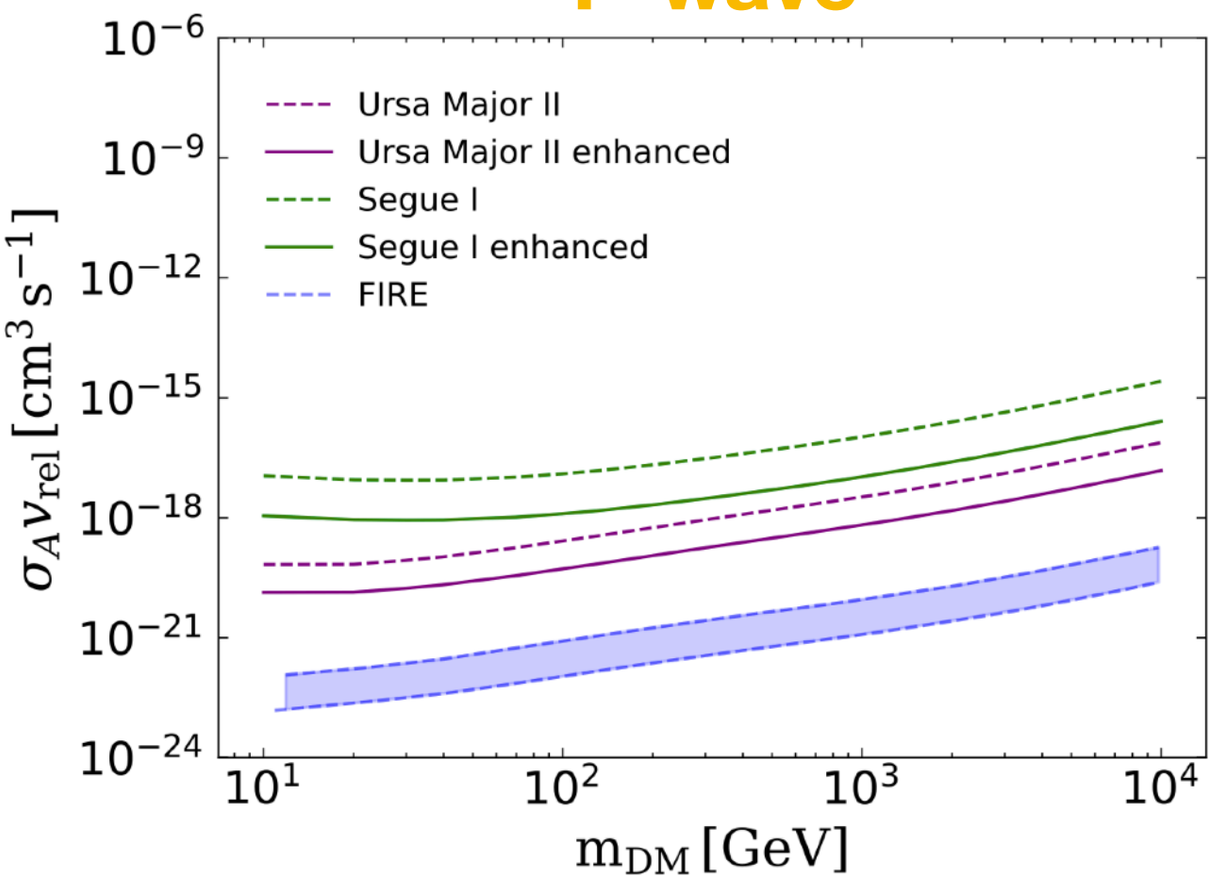

Impact on Exclusion Limits

- Determined the predicted boost for **Ursa Major II** and **Segue I**
- Recomputed **P-Wave** and **D-Wave** exclusion limits, taking into account unbound MW DM particles

P-wave

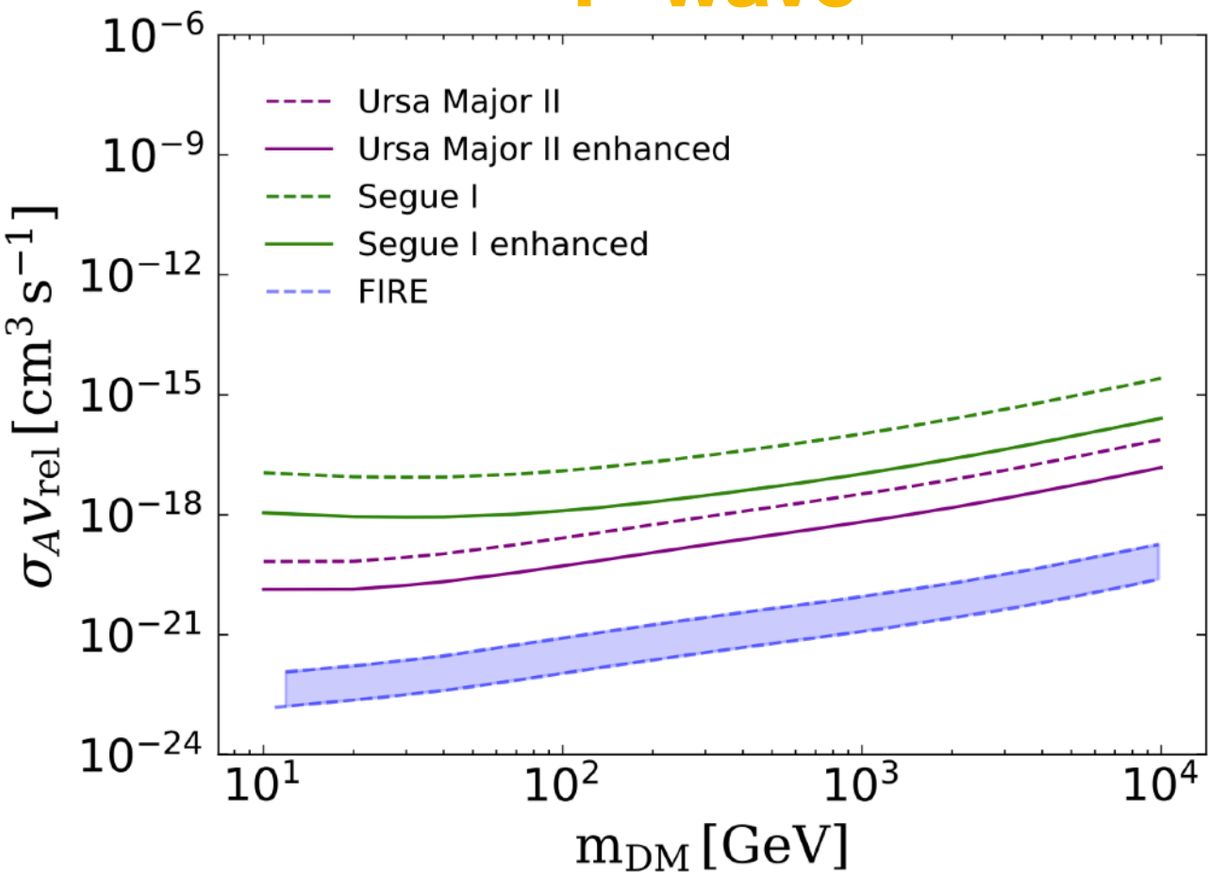

D-wave

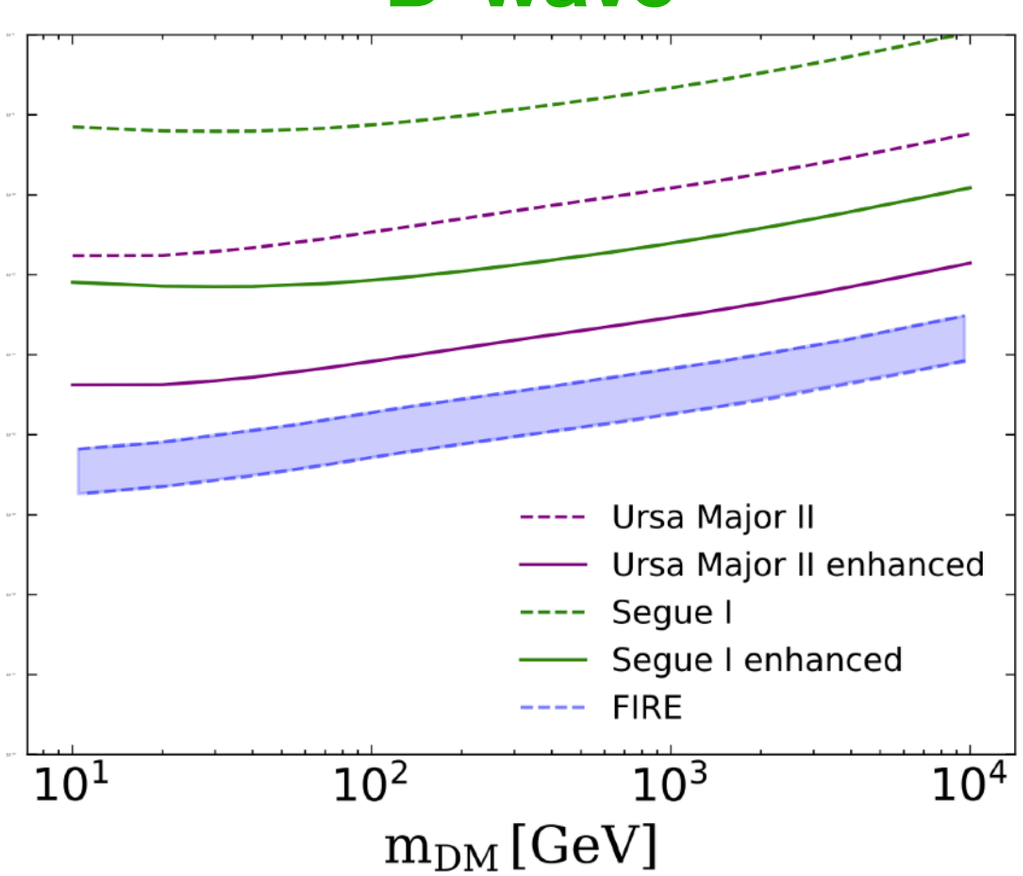

Conclusions

- DM annihilation emission from the MW foreground is larger than the emission from Sgr for all annihilation models except for **Sommerfeld**

Conclusions

- DM annihilation emission from the MW foreground is larger than the emission from Sgr for all annihilation models except for **Sommerfeld**
- Spatial morphology of predicted DM emission from Sgr is likely too extended to explain observed point-like emission

Conclusions

- DM annihilation emission from the MW foreground is larger than the emission from Sgr for all annihilation models except for **Sommerfeld**
- Spatial morphology of predicted DM emission from Sgr is likely too extended to explain observed point-like emission
- Unbound MW DM particles within MW subhalos can boost the expected **P-Wave** and **D-Wave** annihilation rates by up to a factor of $\sim 10^{1.7}$ and $\sim 10^{4.7}$

Conclusions

- DM annihilation emission from the MW foreground is larger than the emission from Sgr for all annihilation models except for **Sommerfeld**
- Spatial morphology of predicted DM emission from Sgr is likely too extended to explain observed point-like emission
- Unbound MW DM particles within MW subhalos can boost the expected **P-Wave** and **D-Wave** annihilation rates by up to a factor of $\sim 10^{1.7}$ and $\sim 10^{4.7}$
- Exclusion limits for Ursa Major III and Segue I are strengthened by ~ an order of magnitude for **P-Wave** and ~ four orders of magnitude for **D-Wave**

Conclusions

- DM annihilation emission from the MW foreground is larger than the emission from Sgr for all annihilation models except for **Sommerfeld**
- Spatial morphology of predicted DM emission from Sgr is likely too extended to explain observed point-like emission
- Unbound MW DM par s can boost the expected **P-Wave** and **D-Wave** annihilation rates by up to a factor of ~ $10^{1.7}$ and ~ $10^{4.7}$
- Exclusion limits for Ursa Major III and Segue I are strengthened by ~ an order of magnitude for **P-Wave** and ~ four orders of magnitude for **D-Wave**

Thank You!

Backups

Sgr J-Factor Profiles (with unbound DM particles)

Bound DM

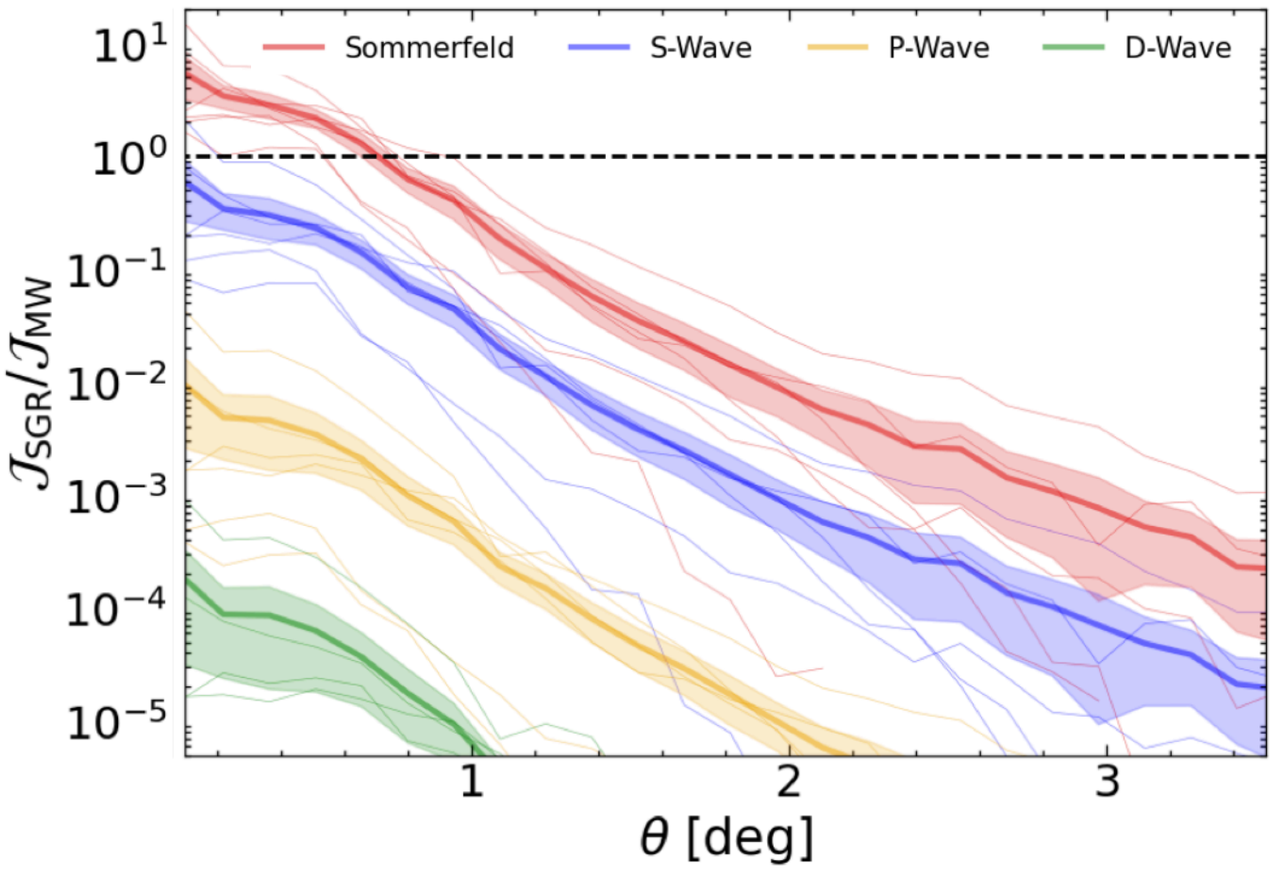

Sgr J-Factor Profiles (with unbound DM particles)

Bound DM

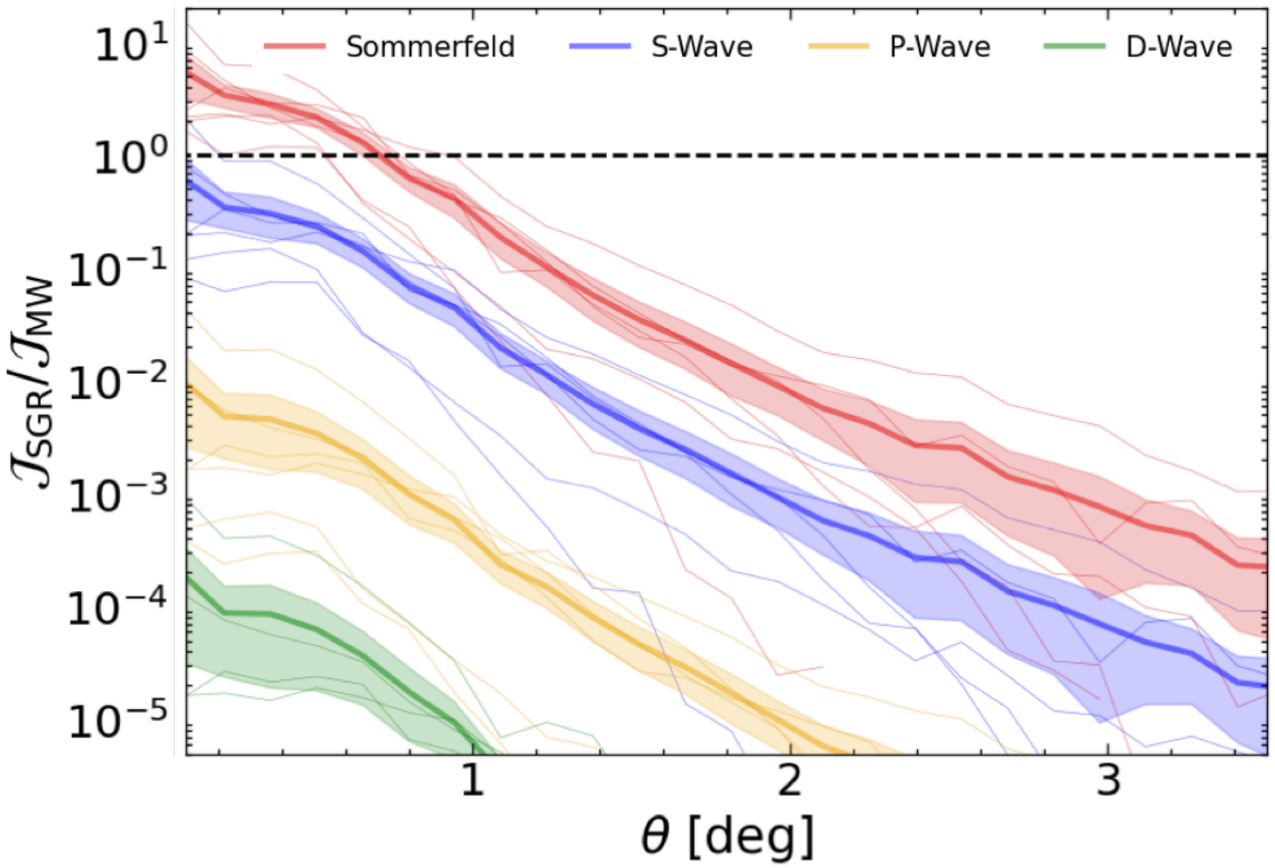

Bound + Unbound DM

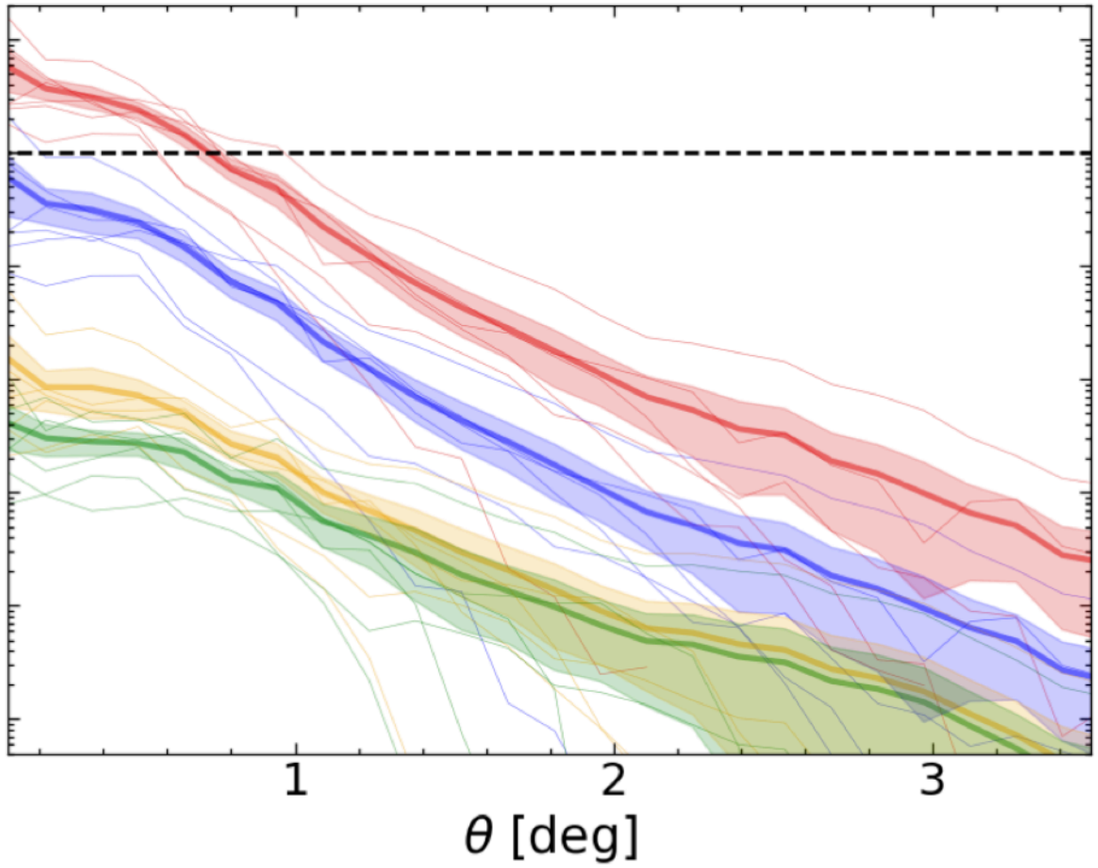

- The unbound DM boosts **P-Wave** by ~ 2 - 30 and **D-Wave** by ~ 20 - 4000

Sgr J-Factor Profiles

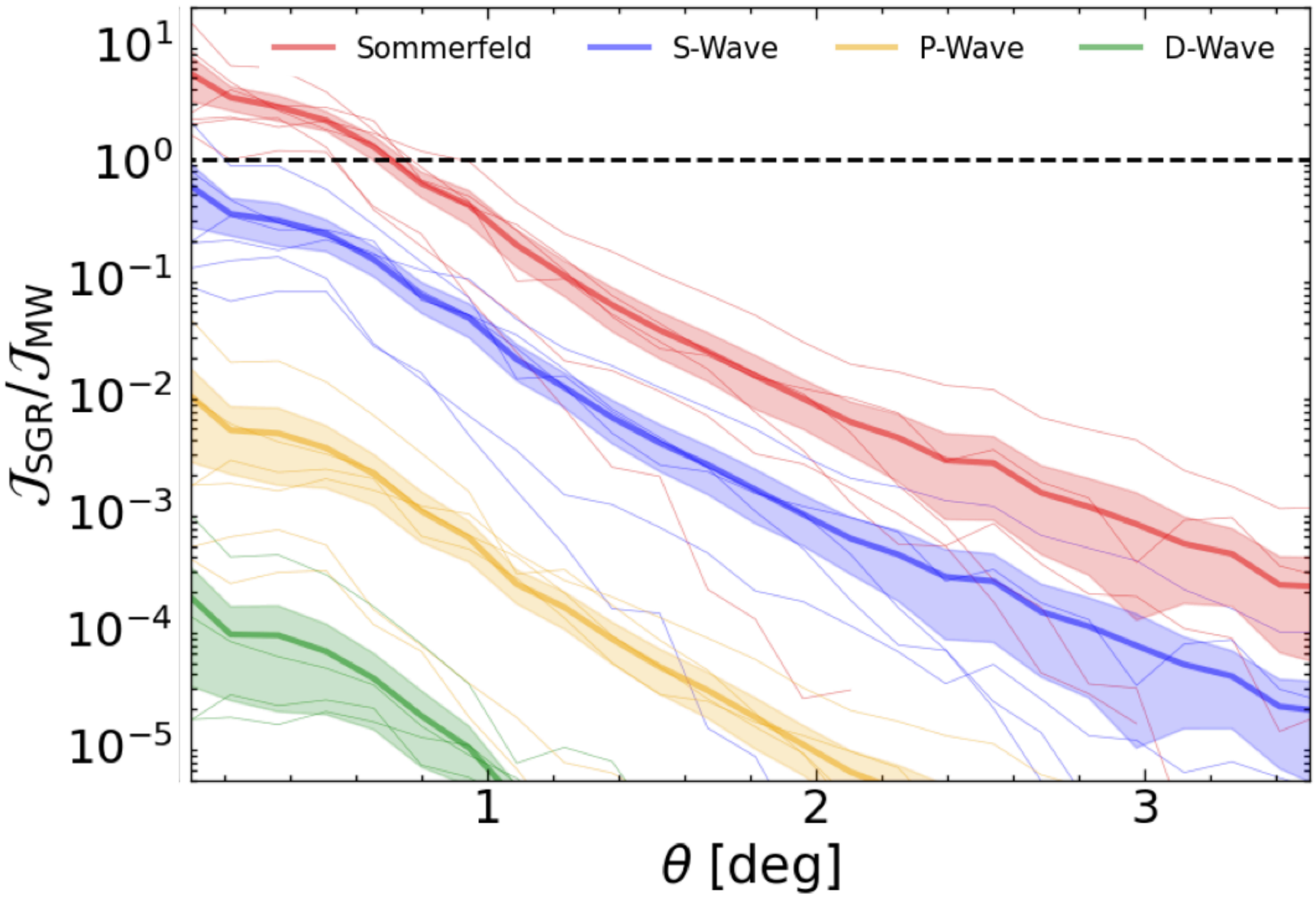

Sgr J-Factor Profiles

- Performed a likelihood analysis using Fermi data
- Angular extension of our model does not fit the observed point-source
- DM interpretation is disfavoured

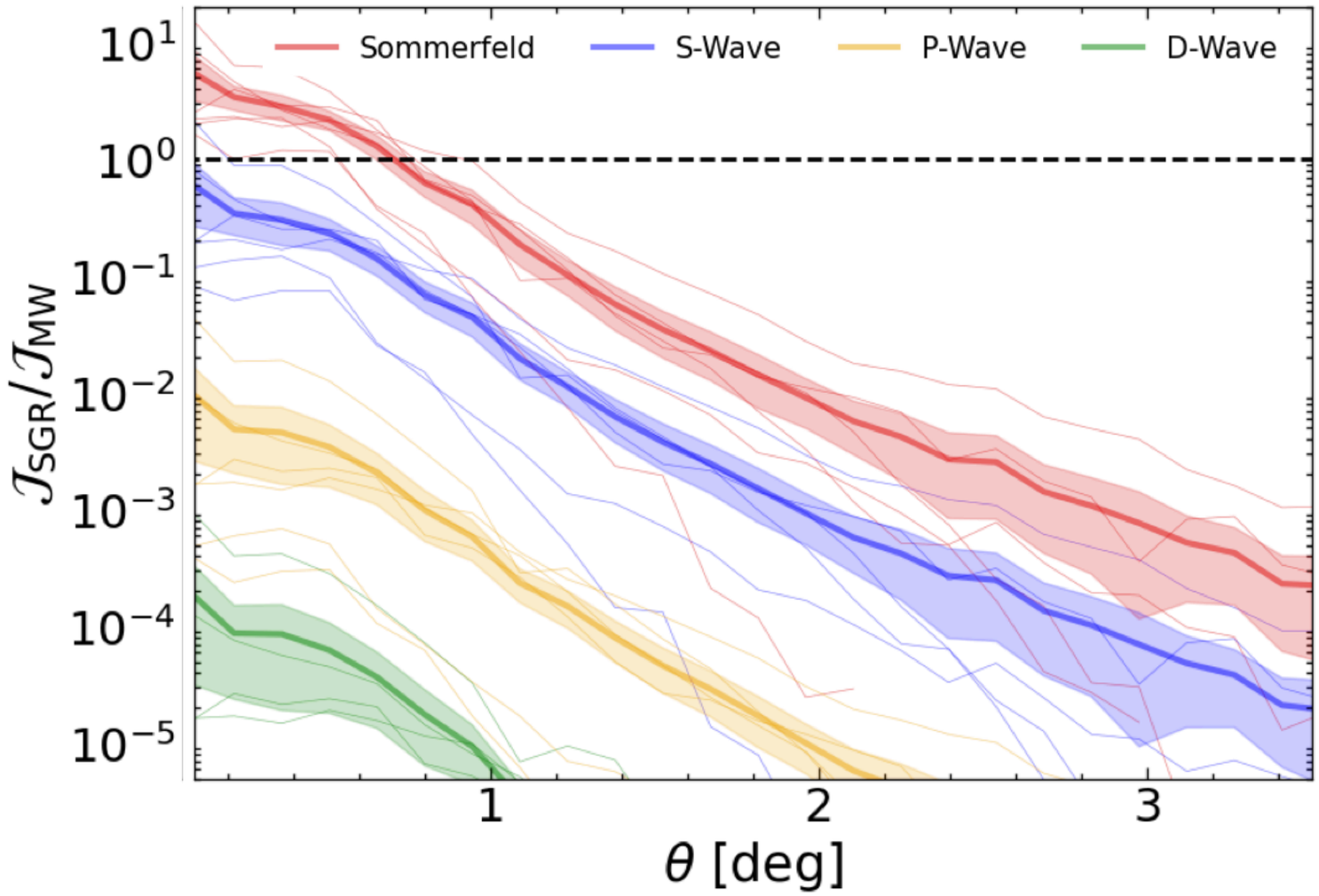

Indirect Detection J-Factor

Smoothhalo

- Local density → voronoi tesselation
- Local relative velocity → interpolation

Sgr Subhalo

- Local density
  - < Rmax → best fit radial density profile
  - > Rmax → voronoi tesselation
- Local relative velocity → average over radial shells

Solar position is selected to match the Sgr's observed position then the l.o.s integral is computed in square bins on the sky

Further Quantifying the Boost

- In a follow up study, we investigated this boost for ~ 900 resolved subhalos from the Auriga simulations

Bound DM

P-Wave

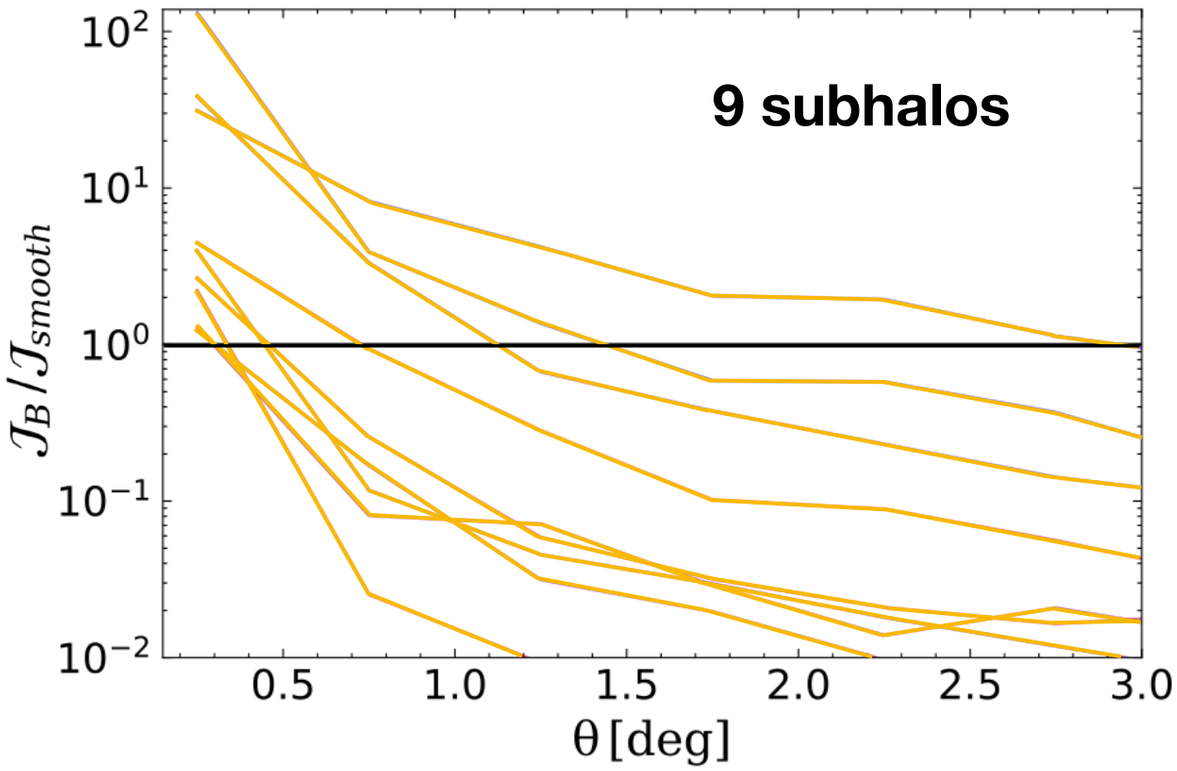

D-Wave

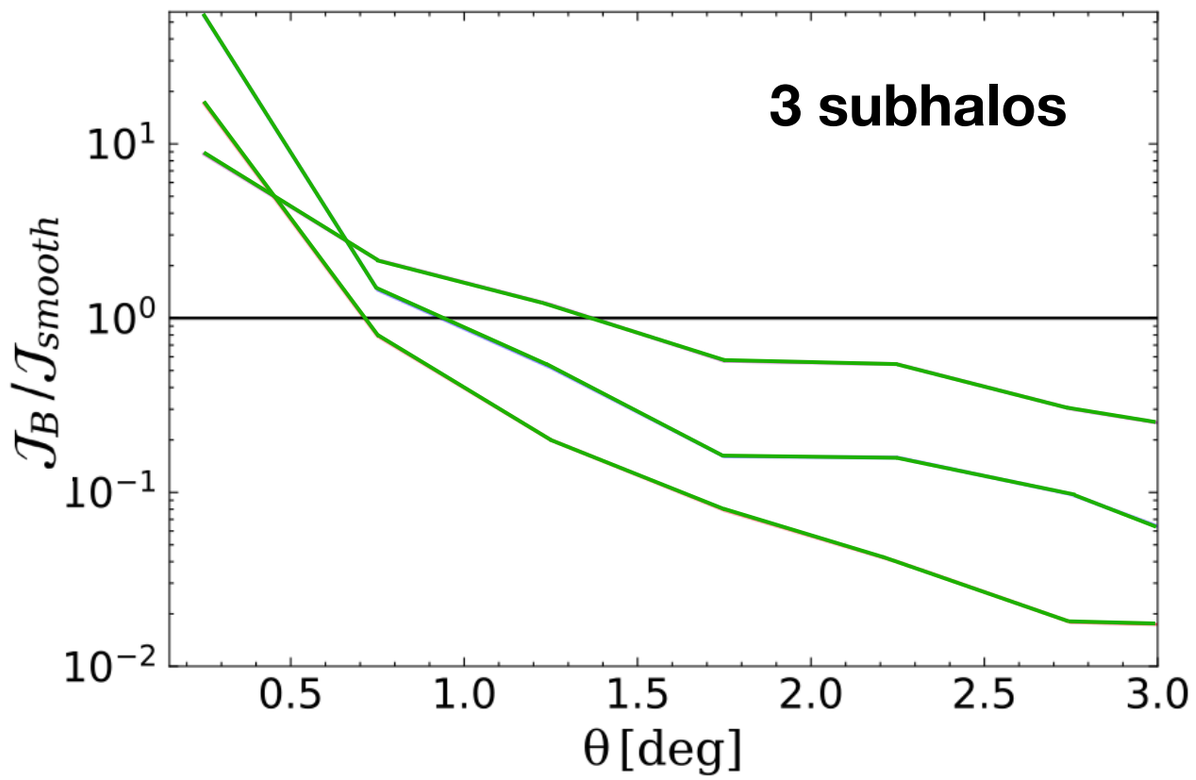

Further Quantifying the Boost

- In a follow up study, we investigated this boost for ~ 900 resolved subhalos from the Auriga simulations

Bound + Unbound DM

P-Wave

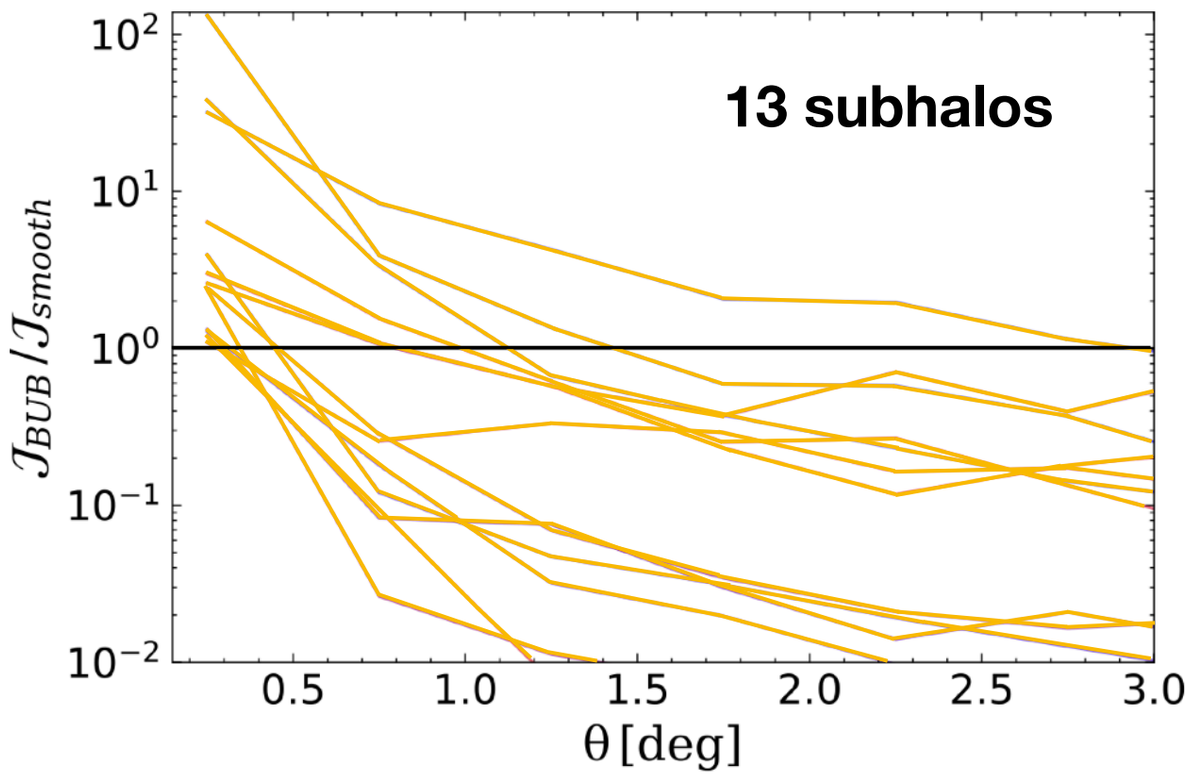

D-Wave

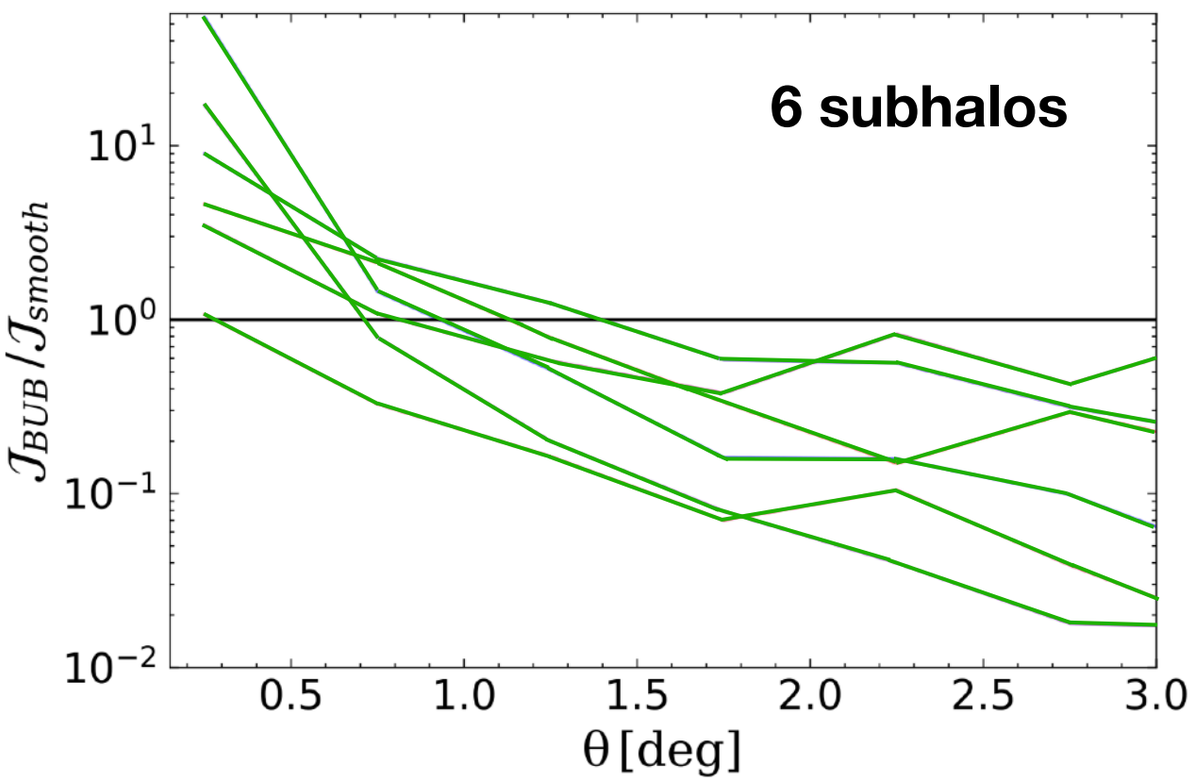

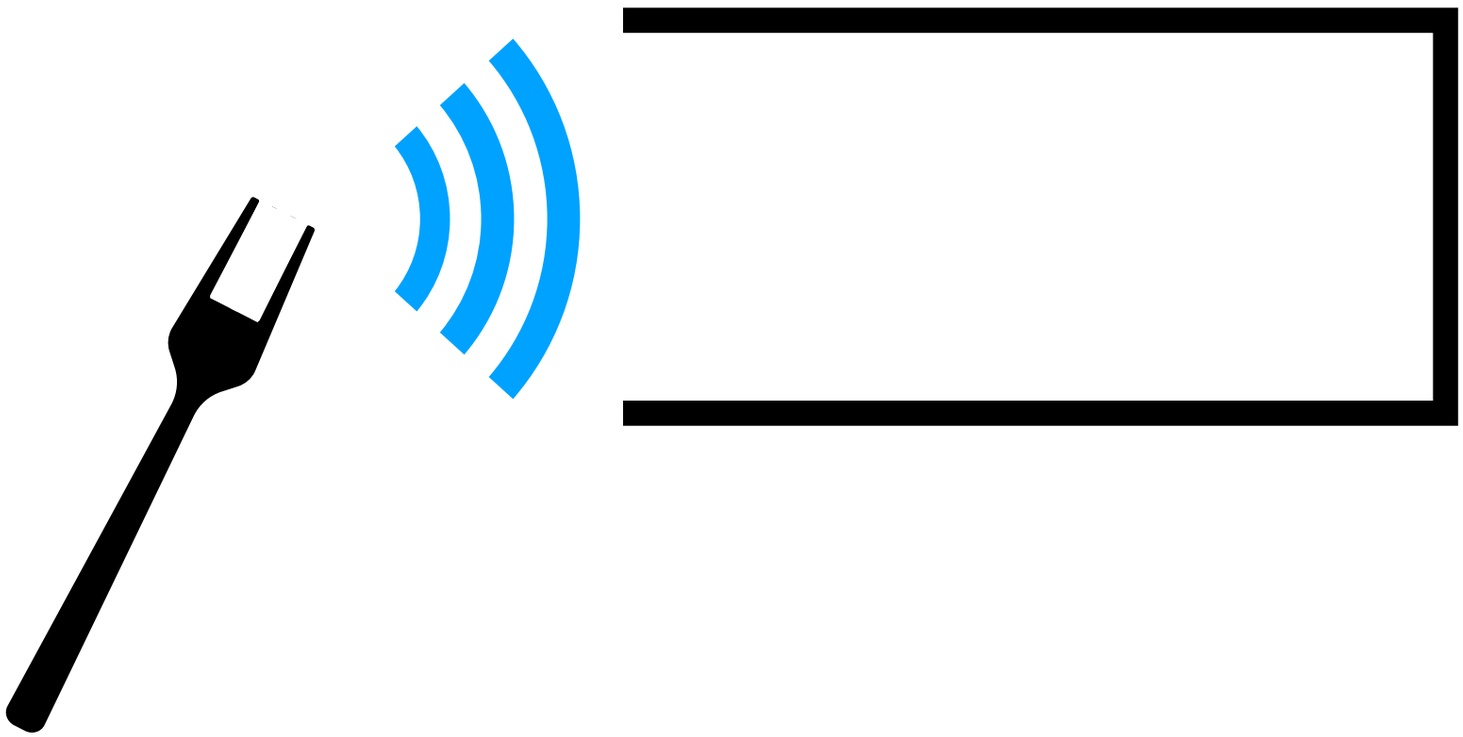

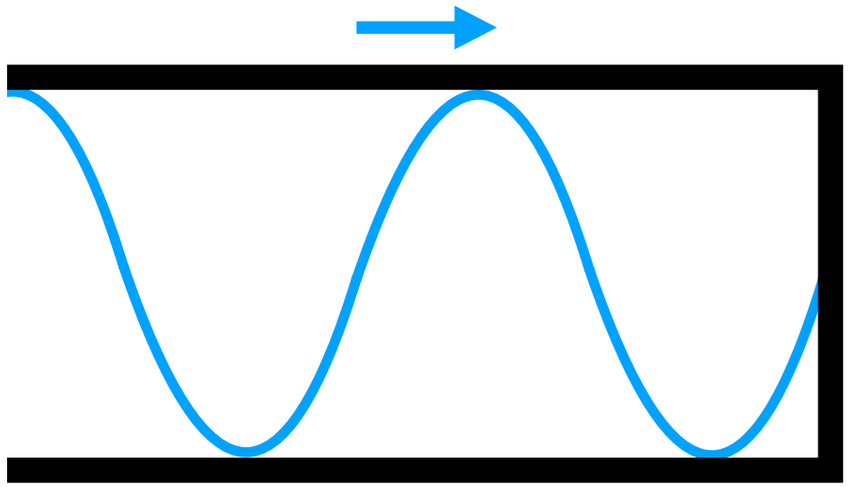

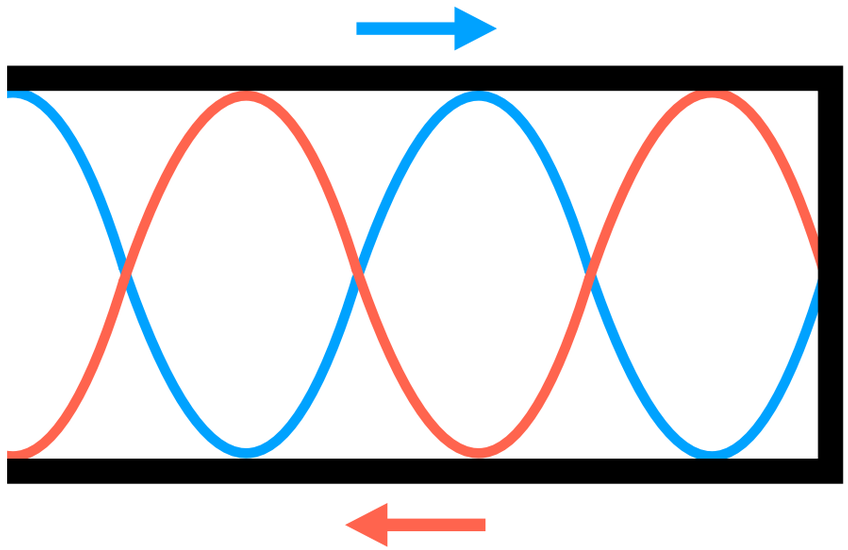

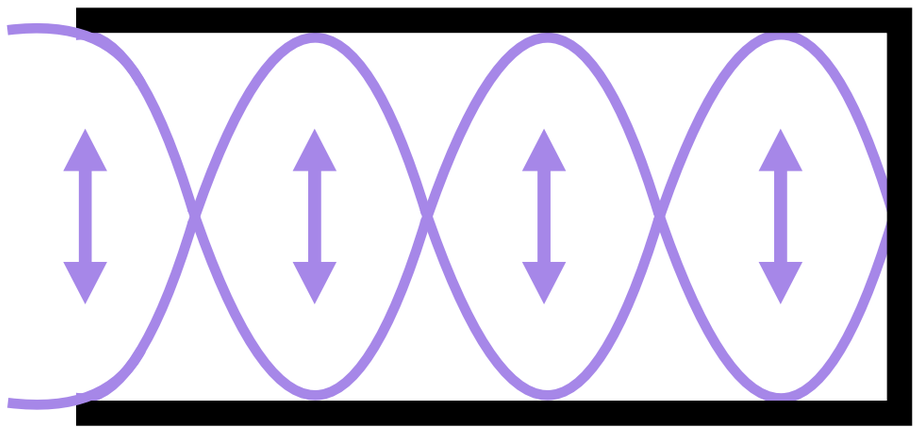

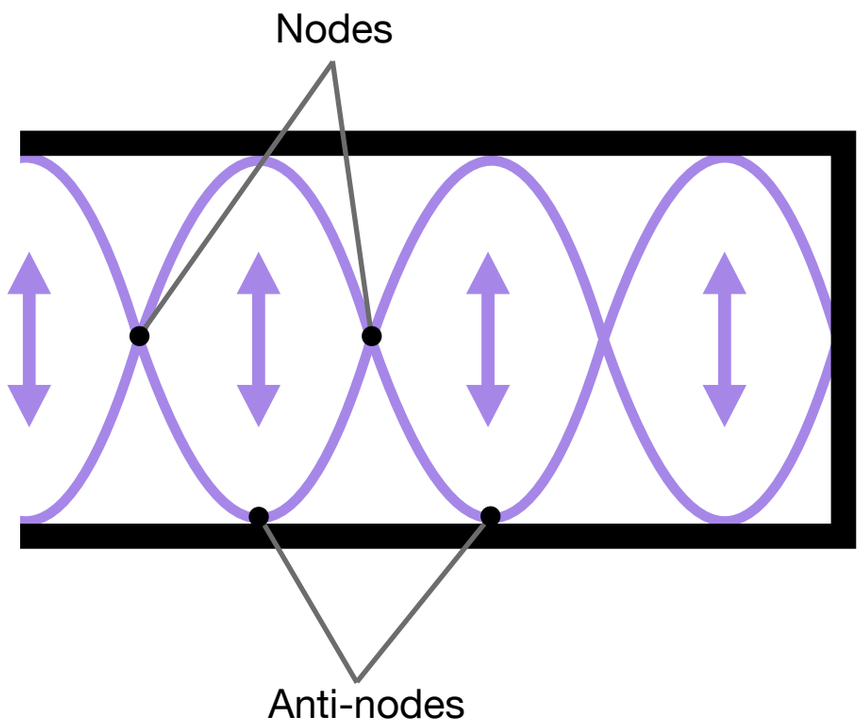
Nodes
Anti-nodes